Rare Earth Elements and Their Behavior During Water Treatment in Nancy, France

A Major Qualifying Project Report

Submitted to the Faculty of

WORCESTER POLYTECHNIC INSTITUTE

In partial fulfillment of the requirements for the

Degree of Bachelor of Science

By:

Matthew Biondi

Matthew Biondi

David Lech

David Lech

Date:

March 1, 2019

Report Submitted to:

Sponsor: Marie-Noëlle Pons (ENSIC)

Advisor: Stephen Kmiotek (WPI)

Acknowledgements

This content and success of this project was made possible by the support of numerous individuals. We would like to recognize their contributions as they were essential to complete this work in a short period of time:

Michelle Adrian for her endless enthusiasm and going out of her way to teach us the French language and culture.

Professor Marie-Noëlle Pons and Professor Stephen Kmiotek for their guidance and knowledge throughout the duration of the project. We could not have achieved the level of experimentation and analysis in this report without their continual support. Thank you, both, for helping us grow as researchers and achieve excellence in our Major Qualifying Project. We would also like to acknowledge the cooperation that established a program between WPI and ENSIC. Our experience in Nancy, France and the travelling that was made possible will be unforgettable. Thank you for organizing this project and for advising our team.

Pauline Louis for her dedication and assistance throughout the project, including operating and troubleshooting the ICP-AES, guiding us through the analysis, and helping us become familiar with the laboratories.

Abstract

Rare Earth Elements (REEs) are gaining significant global demand in multiple development sectors, resulting in greater presence in water sources. Water production and wastewater treatment were two identified processes to aid in removal of these elements. In this study, the effects of different treatment techniques were analyzed for the impact on the following REEs: Ce, Nd, Gd, Tb, and Yb. Commercial and biological activated carbon samples proved to be effective adsorbents for REEs at an optimal dose and time of 125 $mg \cdot L^{-1}$ and 120 minutes, respectively. Activated carbon samples refined from banana and orange peels proved to have a higher adsorption capacity than the commercial alternative. Wastewater treatment processes also proved effectiveness in REE removal, demonstrating nearly 100% removal regardless of the iron (III) chloride dose.

Table of Contents

Table of Tables

Table of Figures

Introduction

Rare Earth Elements (REEs) are gaining exponential attention in modern society, with uses in energy, optics, automotive, and chemical sectors. As a result, global demand for these abundant elements is rapidly increasing (United States Environmental Protection Agency, 2012). From this increase in uses in industrial production, REEs are becoming prevalent in water sources, such as lakes or rivers, as byproducts or through runoff. The health risks associated with REEs, especially heavy REEs, have not been studied in depth. Cerium (Ce), Gadolinium (Gd), and Lanthanum (La) are the only REEs with extensive research performed on their health impacts; and both were determined to be toxic to human health (Pagano et al, 2015).

Depending on its level of contamination, water is generally treated in two different facilities: drinking water production and wastewater treatment plants. In the drinking water production process, safe and sufficient water is produced for drinking, food preparation, and cleaning purposes (The Water Treatment Process, 2019). While this process varies in each plant, activated carbon is generally used as an adsorbent for contaminants during the treatment process, due to its high surface area and pore volume. An adsorbent works by physically or chemically attracting liquids or gases to its surface, including internal surfaces such as pores.

Wastewater treatment plants reduce the concentrations of harmful contaminants to a level at which it can be released back to the environment without adversely affecting human health or the environment (Perlman & USGS, 2016). In Europe, tertiary treatment, the focus of this project, is typically a chemical process to remove superfluous phosphorus from the water (Perlman & USGS, 2016; Peirce et al, 1998). Many of the processes in tertiary treatment utilize iron (III) chloride ($FeCl_3$), as it is proven to be effective at removing nutrients from water (Zhou et al, 2008; DeVries, 2011).

In the Rhine-Moselle Watershed of Northern Europe, studies have found a growing presence of REEs due to anthropogenic sources (Tricca et al, 1998). The main hypothesis accredited to the presence of Gd is the use of Gd in MRI contrast media (Carr et al, 1984; Bau & Dulski, 1996; Ferris & Goergen, 2017; Lerat-Hardy et al 2019). In addition, many chemical production complexes are built around the Rhine (Frijter & Leentvaar, 2003), with large amounts of heavy metals discharged into the river, which may contribute to the presence of REE.

The removal of five REEs in water production and wastewater treatment were explored in this paper: Ce, Nd, Gd, Tb, and Yb. It was determined if activated carbon could be an effective adsorbent for the removal of REEs in water production facilities. In addition, $FeCl_3$ was tested as a chemical agent to remove REEs in wastewater treatment plants.

Background

Rare Earth Elements

REEs are 17 elements on the periodic table that include all of the Lanthanides, as well as Scandium (Sc) and Yttrium (Y). Despite their name, REEs are not rare. They are abundant in nature, but due to their low concentrations in ores, they are difficult to separate and process. Monazite and bastnaesite are two ores found in metamorphic rocks that naturally incorporate light rare earth elements (LREEs) in their composition. The LREEs include lighter lanthanides on the periodic table such as La, Ce, and Nd. There is not an agreed upon definition of a LREE, but generally they have atomic weights less than 158 grams per mole (Geological Survey of Queensland, 2014). Xenotime is another ore commonly found in igneous rocks and the primary source for heavy rare earth elements (HREEs). The HREEs include heavier lanthanides such as Ytterbium (Yb) and Lutetium (Lu). Authors frequently disagree about the classification of lanthanides that are in the center of the spectrum, such a Gd and Terbium (Tb) (Voncken, 2016). The location of the REEs on the periodic table can be seen in Figure 1.

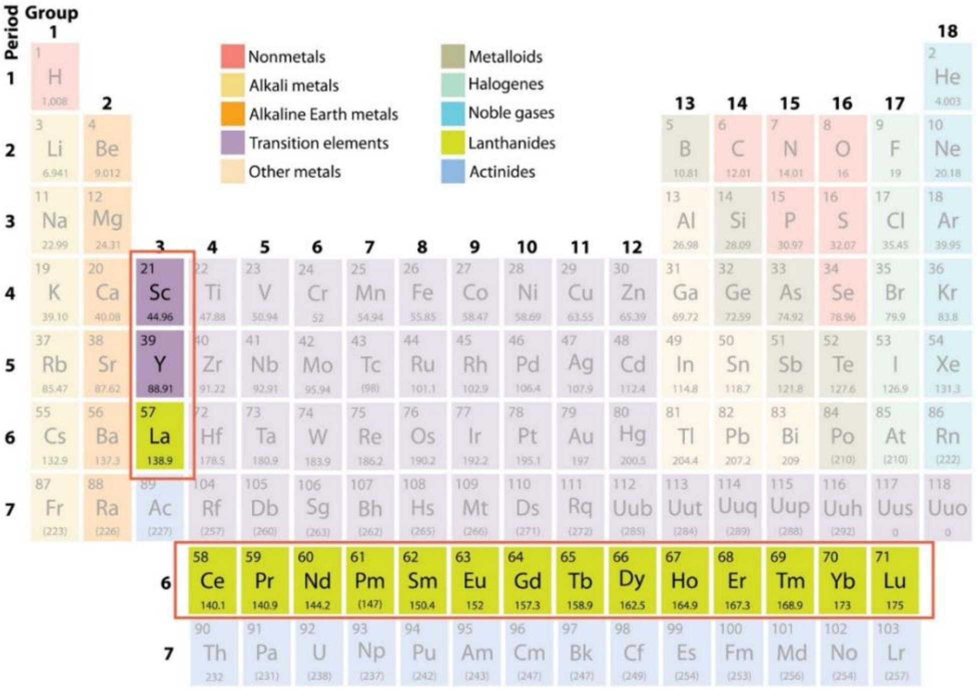

Figure 1: Periodic table with rare earth elements highlighted

REEs are critical components to power electronics, and are used in other sectors including energy, optics, chemicals, automotive, and defense industries. There is an increasing global demand for REEs to use as materials in advanced technologies (United States Environmental Protection Agency, 2012). Exploration and production of these resources will have to expand to accommodate the growing demand. Specific applications for REEs discussed in this report can be found in Table 1.

Table 1: Applications of rare earth elements

Rare Earth Element	**Application**
Cerium (Ce)	Glass polishing agents, fluorescent lamps, catalytic converters, petroleum cracking catalysts, fuel additives
Neodymium (Nd)	Permanent magnets, hard disks, digital video discs, regenerative systems, audio equipment
Gadolinium (Gd)	Televisions, compact discs, computer parts, intravenous radiocontrast agent, scintillator in positron emission tomography (PET) scans, neutron radiography, magnetic refrigeration
Terbium (Tb)	Phosphors in cathode ray tubes, phosphors in liquid crystal displays, fluorescent lamps, televisions
Ytterbium (Yb)	Radiation source in portable x-ray devices, ceramic magnetic devices

Natural anomalies such as La, Gd, and Lu in seawater or Ce and Europium (Eu) in rivers are common (Kulaksız et al, 2013). Evidence suggests that these anomalies can occur based on the geology of the river basin (Goldstein et al, 1988). This was noted near the city of Epinal, as the concentrations of Eu were higher downstream of the river. It is still uncertain whether this was due to natural geographic changes or not. However, there is established and growing evidence of REE contamination and bioaccumulation past this expected baseline. Anomalies of REEs in water sources are being caused by the increasing use and disposal into water sources (Rabiet. et al, 2009). Runoff from agricultural uses, due to REE implementation as fertilizer supplements in China, is an additional source of REEs in water supplies (Gwenzi et al, 2018). REEs may adsorb onto solid sources like sediments, which in turn bring them into streams, estuaries, and finally water and wastewater treatment plants (Gwenzi et al, 2018). Gd is the most common REE by anthropogenic contamination. Gd is used as a contrast agent in magnetic resonance imaging machines (MRIs), thus are quickly released into wastewater systems through humans (Carr et al, 1984; Bau & Dulski, 1996; Bau et al, 2006). However, due to their inert and stable behavior, treatment systems have limited capacity to remove this element before discharging back to the environment (Gwenzi et al, 2018).

While the demand for REEs in manufacturing continues to grow, the health effects of most REEs, especially HREEs, are generally unexplored. La, Gd, and Ce are the only extensively studied REEs monitored for adverse health effects; each was determined to be toxic to human health (Pagano et al, 2015). Other ecological effects by LREEs have been observed in agriculture. An agricultural toxicity study concluded that La and Ce inhibited cell growth and decreased root sizes of onions (Kotelnikova et al, 2019). Studies investigating the effects of heavier REEs on ecosystems are not well-documented, but current trends have raised concerns for those dependent on contaminated water sources.

Rhine-Moselle Watershed

The Rhine River is one of Europe's best known rivers and among the most important. Beginning in Switzerland, it flows through France, Germany, the Netherlands, and into the North Sea. The 200,000 km^2 watershed supports agriculture across Europe and provides potable water to over 20 million Europeans (Frijters & Leentvaar, 2003; Uehlinger, 2009). The pH of this river is neutral to slightly alkaline, measuring between 7.5 and 8.5 between seasons (Uehlinger, 2009; Hommen & Rudel, 2012). The Rhine is also the most densely populated shipping route in Europe. It connects the world's largest inland port in Duisburg, Germany to the world's largest shipping port in Rotterdam, Netherlands. Tributary rivers expand access and navigable connections to the Rhine. Among the most important tributaries, and the one that will be sampled from in this report, is the Moselle River. The Moselle is the longest tributary to the Rhine and, similarly, is important for providing agricultural water supply, potable water, and ship routes (Frijters & Leentvaar, 2003).

Despite its use as a water supply for agriculture and drinking, there is a surprising history of REE contamination from anthropogenic sources. Vast industrial complexes are built around the Rhine, making up most of Europe's chemical production (Frijters & Leentvaar, 2003). The river basin is an advantageous location to build industries because of nearby ports for quick product shipping. Moreover, these industries use the river to dispose of industrial waste up to a certain limit. Several large cities around the river also contribute contamination by medical devices or direct waste disposal to the river. The largest medical contamination is Gd, resulting from its use as a contrast media in MRIs. The REE media is injected into patients before an MRI and excreted by the body within 24 hours, directly entering public wastewater treatment from toilet waste. Studies have shown a significant presence of Gadolinium in water sources that may be attributed to MRIs (Bau & Dulksi, 1996; Bau et al, 2006; Rabiet et al, 2009; Lerat-Hardy et al, 2019). A map of the Rhine, Moselle, and major cities can be found in Figure 2.

Figure 2: Map of the Rhine River (yellow), Moselle River (orange), other tributaries (blue), and major cities

Water Production

The goal of the water production process is to produce a safe and sufficient supply of water for drinking, food preparation, hygiene, and cleaning (Drinking Water, 2018). Water treatment plants bring in surface or groundwater of varying contamination levels and treat it accordingly to become potable. Certain water production plants, as mentioned later on, maintain secrecy of their processes for security reasons. However, in a typical water production plant, flocculation, filtration, and disinfection prepare the water for distribution to the given population (The Water Treatment Process, Retrieved January 2019).

A supplemental step in the water production process is adsorption with activated carbon, an adsorbent with use dating back to 450 BC in Hindu documentation (Çeçen & Aktaş, 2012). By the early 20th century, activated carbon developed presence in water treatment facilities, to remove odor, color, and disinfection by-products. Characteristics such as high surface area, pore size, and density allow adsorption of a variety of different contaminants to its surface (Dvorak & Skipton, 2013). Applications for activated carbon are growing, as a wider range of pollutants enter the hydrosphere through human activity.

Commercial activated carbon (CAC) is mainly produced from bituminous coal, coconut shell, and wood (Calgon Carbon, 2012). Bituminous coal is transformed into activated coal by devolatilization, followed by activation with steam or oxygen (Akash & O'Brien, 1997). Activated carbon from agricultural waste sources, such as peels from various fruits and coconut shells require more refining than the coal to produce the same quality substance with equal or greater pore volume. Various experiments have found it possible to produce activated carbon with the banana peels (Kadirvelu et al, 2003; Mohammed & Chong, 2014; Kusrini et al, 2018). Utilizing different raw materials for production results in different characteristics of the final product, such as varying surface area and pore volume. Banana peels are a more desirable choice for production because despite the additional refining required, banana peels are more environmentally friendly, as the banana tree is not killed to harvest the fruit.

One of the newly tested applications of activated carbon adsorption is for the removal of heavy metals, such as REEs. With an increasing demand for REEs in modern technology, they are becoming more prevalent in water supplies (Kano et al, 2017). The removal and recovery of these heavy metals is important from both an environmental protection and a resource recovery standpoint. Recent studies have concluded that activated carbon has the capacity to remove REE from water samples (Kano et al, 2017, Kusrini et al, 2018).

Wastewater Treatment Plant

Wastewater treatment plants (WWTP) perform with the goal of reducing the concentrations of harmful pollutants to the level at which it can be released back into the environment without adversely affecting human health or the environment (Perlman & USGS, 2016). Wastewater treatment occurs in three distinct stages, each with different objectives, laid out in Table 2. In small scale testing, temperature of treatment and pH are typically considered, as both are essential parameters in the optimization of chemical processes (Gabor, 2017). However, WWTPs operate using millions of gallons of water per day, so the temperature and pH are not altered during treatment. A simplified version of the wastewater treatment process can be found in Figure 3.

Table 2: Treatment stages and objectives in wastewater treatment plants

Treatment Stage	Objective
Primary	Physical removal of suspended solids and some biochemical oxygen demand (BOD)
Secondary	Biological removal of BOD
Tertiary	Physical, biological, and chemical removal of nutrients and inorganic pollutants, such as REEs

Primary Treatment

Primary wastewater treatment is effective in removing about sixty percent of suspended solids and around 30 percent of BOD from the influent (Peirce et al, 1998; Perlman & USGS, 2016; Lenntech, n.d). Influent water is screened through bars then pumped through a grit chamber to remove or break down any large materials that may cause damage to the equipment in the later stages of treatment (Peirce et al, 1998). The water then moves into the primary settling tank, where the larger particles and organic matter settle to the bottom of the tank over 24 hours.

Secondary Treatment

After primary treatment, the wastewater no longer contains a majority of the suspended solids, but it still contains a large portion of nitrogen and BOD; an indirect measurement of the amount of organic material in water. Secondary treatment focuses on this removal, typically through an aeration tank with activated sludge, or with biofilters. In an aeration tank, water flows through activated sludge from the primary clarifier along with microorganisms. Sludge from the clarifier is pumped to the tank as it contains microorganisms which are in an environment without food, and are ready to consume dissolved organic matter (Peirce et al, 1998). Additional oxygen is added to the aeration tank to provide sufficient oxygen for the aerobic processes. A biofilter consists of a bed full of "fist-sized" rocks, home to active microbial growth (Peirce et al, 1998). Water is pumped from beneath the filter bed and, like an aeration tank, the microbes consume the organic matter present in the influent water. Secondary treatment is responsible for the removal of over 85 percent of nitrogen, 95 percent of suspended solids, and over 90 percent of BOD (Peirce et al, 1998; Zhao et al, 2013; Perlman & USGS, 2016).

Tertiary Treatment

The effluent of secondary treatment is still polluted with nutrients and toxic substances (Pierce et al, 1998). Tertiary treatment is important for the removal of excess BOD, organic, and inorganic substances. Processes involved in this stage of treatment can include disinfection, oxidation, coagulation and filtration, or reverse osmosis (Muralikrishna & Manickam, 2017).

Coagulation is very effective at removing dissolved material from water, such as inorganic particles and nutrients such as phosphorus. $FeCl_3$ is the most common coagulant used in water or wastewater treatment. $FeCl_3$ is effective at removing excess phosphorus from water sources (Zhou et al, 2008; DeVries, 2011). Currently, its ability to remove REEs from wastewater is not heavily researched.

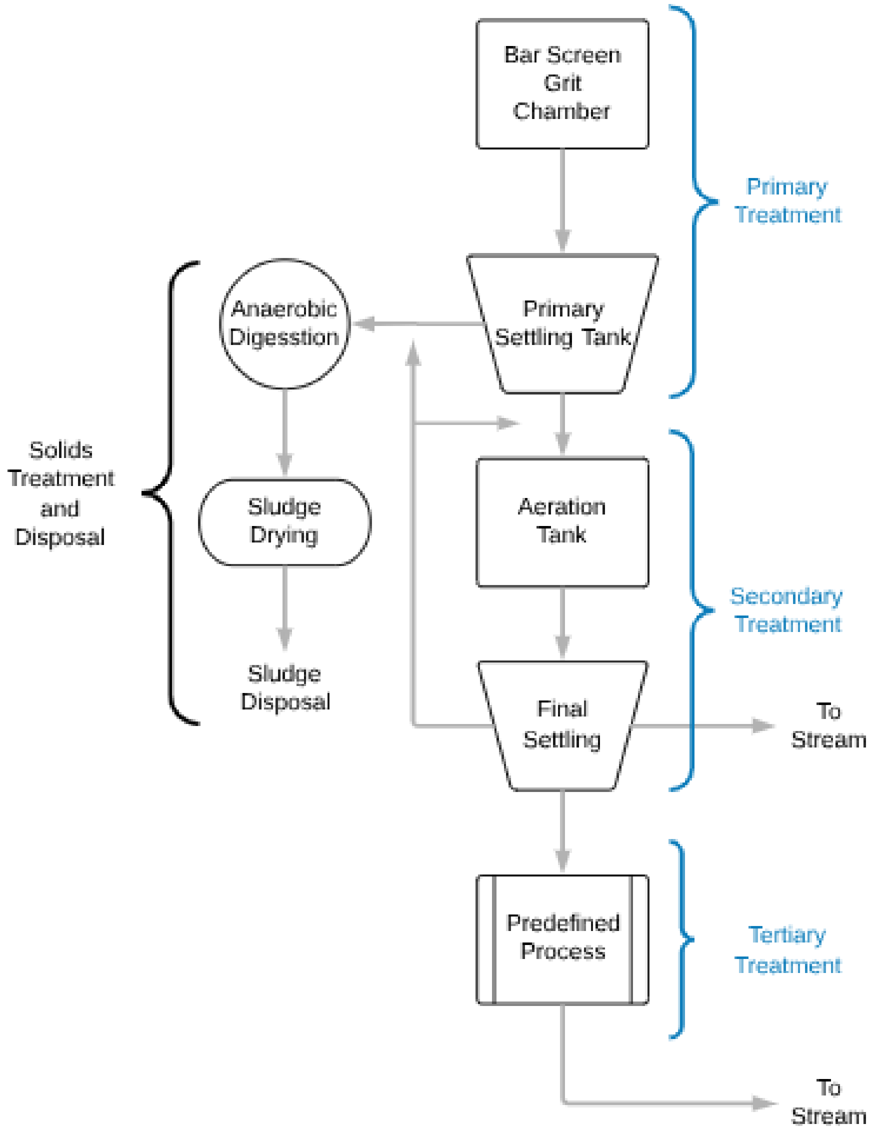

Figure 3: Process flow diagram of wastewater treatment plants

The Grand Nancy WWTP operates in Nancy, France, treating the wastewater of the 350,000 inhabitants of the metropolis. This treatment facility operates very similarly to the process as described above. The tertiary treatment at this plant is primarily focused on the removal of excess phosphorus with $FeCl_3$. This is essential, as excess nutrients in surface water can be harmful to the ecosystem.

Methodology

Chemicals and Reagents

A Moselle River sample for water production absorption tests was collected near the intake point for Nancy drinking water production. Stock solutions at different concentrations were prepared from gadolinium (III) nitrate hexahydrate (Sigma-Aldrich), cerium (III) nitrate hexahydrate (MilliporeSigma), terbium (III) chloride hexahydrate (Sigma-Aldrich), neodymium (III) nitrate hexahydrate (Sigma-Aldrich), and ytterbium (III) chloride hexahydrate (Sigma-Aldrich) in deionized ultrapure water. Sodium hydroxide (NaOH) was used to prepare the biological activated carbon (BAC). The adsorbents used in the water production study include a CAC called Acticarbone (CECA) as well as BACs produced from banana and orange peels.

Wastewater samples were collected from the effluent of the secondary treatment step of the Grand Nancy WWTP. A synthetic wastewater stock solution was also made to complete the study without microbial influences using wastewater composition data in Appendix C Table C.1. The stock was prepared with Calcium carbonate (R.P. Normapur), Magnesium sulphate heptahydrate (Merck), Sodium chloride (Prolabo), Potassium nitrate (Rectapur), and Dipotassium phosphate (Fluka-Garantie). The coagulants used in the WWTP include iron (III) chloride hexahydrate (Acros Organics), fine sand, and Floerger® AN 923 VHM anionic polymeric flocculent.

Lab Safety

Before entering the lab, a mandatory safety training course was completed with a safety instructor at ENSIC. Then, general laboratory safety was taken into consideration for every experiment. This required wearing a lab coat, safety glasses, long pants, and closed toe shoes. No food or drinks were permitted in the lab. In addition to these safety requirements, there were safety considerations that were specific to our experiments. The primary safety concern involved work with hazardous chemicals such as

REEs, acids, and bases. To ensure that we followed the relevant safety procedures when working with these chemicals, the bottle labels and material safety data sheets were referred to for each chemical.

NaOH is strong base that could be fatal if ingested; it can cause severe irritation to the skin, eyes, and the respiratory tract (Central Drug House, n.d.). Special storage cabinets isolated from other chemicals will be used for bases in the lab. Ce, Nd, and Yb are REEs that are toxic to human health and can cause acute irritation to the skin, eyes, and respiratory tract (Central Drug House, n.d.). Gd and Tb are other REEs that can also cause acute or serious irritation to the skin, eyes, and respiratory tract, but their toxicity to humans is not well documented (Pagano et al, 2015).

Preparation of Biological Activated Carbon and Biochar

Procedures from Mohammed & Chong (2014) and Kusrini et al. (2018) were evaluated for the production of BAC from banana peels. The experiments performed by Kusrini et al. (2018) aligned with our goals more directly, so that procedure was followed in testing, with additional assumptions gathered from Mohammed & Chong (2014). Orange peels have also been tested for the production of activated carbon, so the following procedure was followed for banana peel activated carbon (BPAC) and orange peel activated carbon (OPAC) in separate batches to produce two BACs.

First, banana peels (*Musa acuminata*) and orange peels (*Citrus reticulata* & *Citrus x sinensis)* were gathered and cut into 1-2 cm pieces. The peels were twice washed: initially with tap water and secondly with deionized ultrapure water. The pieces were dried in the oven at 110°C for 24 hours. They were then pulverized in a mill blender to a uniform size of 250 µm. The fragments were then carbonized in a furnace at 400°C for 1 hour, then cooled until they reached room temperature. Then, the material was left in a 45 percent NaOH solution at a ratio described by Mohammed & Chong (2014) of 4:1 NaOH to carbonized material for 16 hours at room temperature. The 45 percent NaOH solution was obtained by putting 45g of NaOH (pellet form) into a 100 mL volumetric flask with deionized ultrapure water until a total volume of 100mL was reached. The resulting solution was filtered with a 20 µm coffee filter, and the remaining residue was dried in the oven at 110°C for 24 hours. The material was then placed in a furnace at 500°C for 1 hour. The material was washed and filtered using deionized ultrapure water until a pH of 7 was obtained. Finally, the material was dried in the oven at 110°C for 8 hours. The resulting BAC was used in the later testing.

Banana peel biochar was produced by Yann Le Brech from the pulverized banana fragments. After pulverization, the powder was placed in a furnace at room temperature. The furnace was heated to 500°C with a temperature increase of 10°C per minute. The powder then stayed in the furnace at 500°C for one hour under 500 normal mL • min^{-1} of nitrogen gas.

Water Production Experiments

The effect of dose and type of activated carbon was measured in batch experiments, along with varying concentrations and mixtures of REEs. Both a CAC and BAC from banana and orange peels were tested as adsorbents. Stir tables were used to keep the mixing rate constant at 250 rpm. The mixing time for prepared solutions was 60 minutes to dissolve the REEs completely, measured at 3,000 µg • L^{-1}. The proper concentration was obtained by measuring a stock solution using mass balance on the given REE salts. Various doses of activated carbon were tested to determine an optimal dose where the activated carbon is not in surplus to remove all of the REEs. The mixing time for optimal adsorption was determined by measuring the adsorption at 15, 30, 45, 60, 120, and 180 minutes and selecting the time at which there was no significant changes in REE concentration for most samples. The concentration was measured using inductively coupled plasma atomic emission spectrometry (ICP-AES) and inductively coupled mass spectrometry (ICP-MS) when river water was present. This was repeated for all REEs in this study, which consist of Ce, Nd, Gd, Tb, and Yb. The longest adsorption time was chosen as the optimal experimental duration for all REEs.

The effects of a mixed REE solution were then tested to determine favorability of adsorption onto the activated carbon. Three REEs, one LREE, one HREE, and one with an intermediate atomic weight, were mixed together at 1 mg • L^{-1} each.

Characterization of Activated Carbon and Biochar

A Scanning Electron Microscope (SEM) was used to visually analyze the pore size and distribution of the CAC, BACs, and biochar. In addition, this provides insight to the density of pores and the relative surface area available for which contaminants to adhere.

Energy Dispersive X-Ray (EDX) analysis was performed on each activated carbon sample. This analysis provided elemental identification within each carbon sample to allow for further comparison between the BACs and CAC.

The adsorption capacity for CAC, BPAC, OPAC, and banana peel biochar were quantified by equation 1:

$$Q_c = \frac{\left(C_i - C_f\right) V}{m} \tag{1}$$

Where Q_c is the REE adsorption capacity of the adsorbent [mg of REE • mg of adsorbent $^{-1}$], C_i and C_f are the initial and final concentration of REE [mg • L^{-1}], respectively, V is the volume of the solution [L], and m is the weight of the adsorbent [mg]. A higher adsorption capacity is desirable, as this means less carbon is required to reduce the concentration of REE in solution.

Wastewater Treatment Experiments

Jar testing was used to test $FeCl_3$ in different small scale scenarios for simulated wastewater treatment. Jar tests mimic the treatment processes of rapid mixing, coagulation and flocculation, and finally settling, in an experimental setting. Dose of $FeCl_3$ and mixtures of REEs were evaluated parameters. Each test was performed with six, 800 mL capacity beakers, with a rapidly mixed coagulation period at 250 rpm for 3 minutes, followed by a slow mixing flocculation period at 50 rpm for 7 minutes, and finally a settling period of 30 minutes with the paddles turned off. Experiments were performed for individual REEs as well as mixtures to identify selectivity of settling in solution. The first set of experiments was performed using 800 mL of synthetic wastewater to avoid microbial influences, followed by experiments with 800 mL of actual wastewater.

The synthetic wastewater was fabricated in accordance with research performed by Louis (2017). A 1,000 mL capacity volumetric flask was filled about halfway with deionized ultrapure water, and put on a stir table with a magnetic stir bar. Sodium (Na), calcium (Ca), magnesium (Mg), and potassium (K) were added in doses as described by the wastewater composition raw data in Appendix C Table C.1. Anion concentrations, such as phosphates, chlorides, and sulfites were also measured, and remained in the same magnitude as the actual wastewater composition. The solution was stirred until a homogeneous mixture was achieved; adding additional deionized ultrapure water as needed. The volume was then brought to 1 L using the deionized ultrapure water. The subsequent tests were performed with this water as follows.

The effect of dose of $FeCl_3$ was tested with constant REE concentration, temperature, and pH. Jars 1-6 were dosed with 0, 1, 2, 3, 4, and 5 $mg \cdot L^{-1}$ $FeCl_3$ respectively at a neutral pH, room temperature, and REE concentration of 3 $mg \cdot L^{-1}$. In addition, 1 $mL \cdot L^{-1}$ of 1 $g \cdot L^{-1}$ Floerger® AN 923 VHM solution and 1 g of fine sand were added to each jar to aid in the coagulation process. From this, the maximum adsorption levels were determined and an optimal dose was obtained.

Results and Discussion

REE Concentration versus Time

Initial experiments were organized to understand the behavior of REEs in containers over time. A test was conducted to measure the uncertainty of results from the ICP-AES by testing samples of the same solution with a Ce concentration of 3,000 $\mu g \bullet L^{-1}$. Two separate batches were prepared using strictly glassware or plasticware to determine if there was any effect from the material of the storage container as well. This was done because silica infused activated carbon and other silica based materials are another method to adsorb REEs (Iftekhar et al, 2018). Borosilicate lab-grade glass is primarily composed of silica and could potentially lower the expected concentration of the samples by adsorbing REEs to the surface of the container. Data collected from the glass versus plastic experiments can be seen in Figure 4.

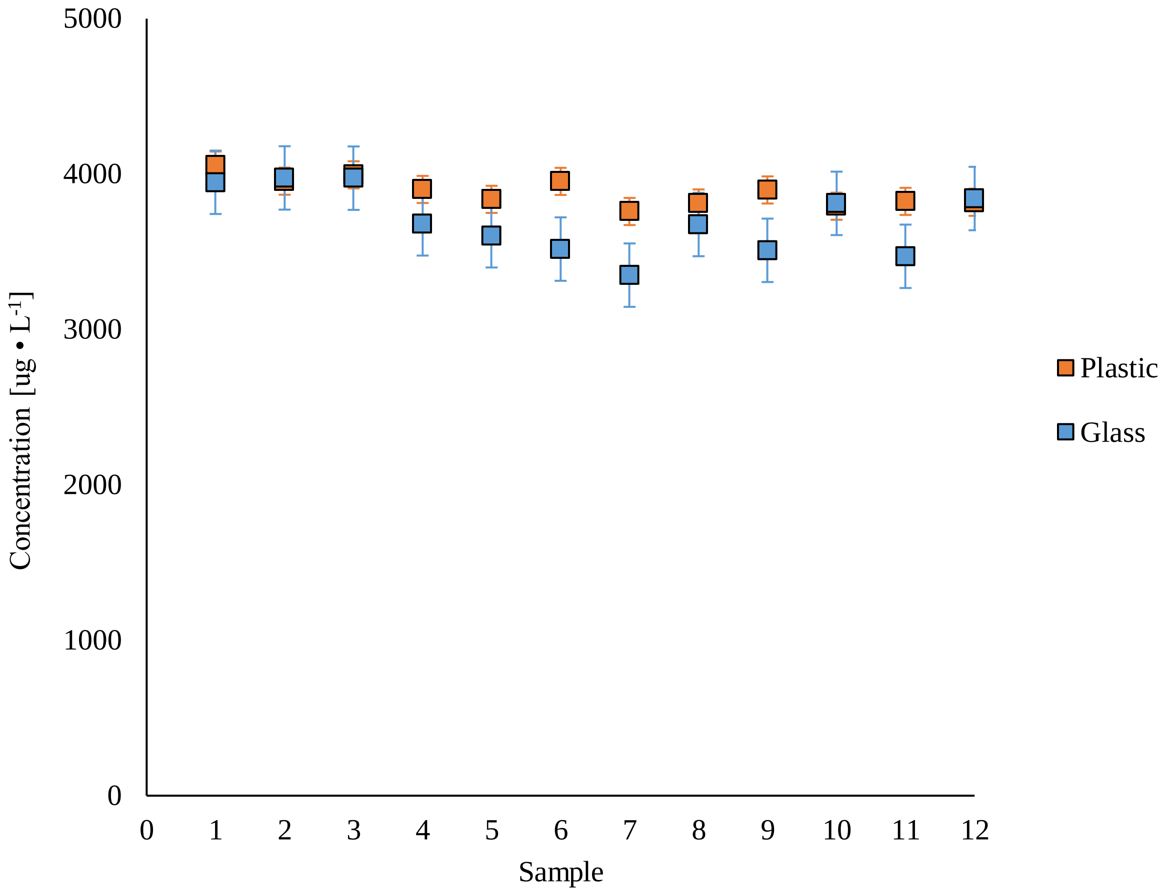

Figure 4: Concentrations of identical Ce solutions made with ultrapure water and prepared using volumetric flasks and storage containers constructed of different materials

Measured concentrations, based on ICP-AES, were between 3,350 and 3,975 µg • L^{-1} with an average of 3,696 ± 204 µg • L^{-1} for solutions prepared with glass materials and the plastic bottle values ranged between 3,759 and 4,058 µg • L^{-1} with an average of 3,884 ± 87 µg • L^{-1}. The standard deviation in the glass bottles was much higher than in plastic bottles, showing higher variability of REE concentration with glass. However, all values were significantly higher than the expected 3,000 µg • L^{-1} concentration, potentially due to an error in preparing the stock solutions at a higher concentration and diluting them to the desired concentration. 75% of the glass bottle samples showed lower concentrations than plastic bottles, with 25% showing statistical significance of lower concentrations, which may be a result of the REEs adsorbing to the walls of the container. The statistical significance in a concentration change appeared to occur more frequently over time, as samples were prepared in order from sample 1 to 12, so the last sample had a longer residence time in the container. This may suggest that adsorption to walls of the material occurs instantly, and continues over time for solutions kept in storage, such as stock solutions or samples in test tubes. Initial concentrations throughout this section may show variability from the desired concentrations for this reason. Solutions were prepared with stocks that ranged in age from 0-14 days and were not always tested immediately after they were prepared, which can cause the initial concentration to decrease over a longer period of time. Each transfer of the solution to a new container could start the adsorption process again and continue to reduce the concentration.

Time was a controlled variable in a secondary experiment to validate a downward trend from REE adsorption to the surface of the preparation material. Two 3,000 $\mu g \bullet L^{-1}$ Nd solutions were made using glassware and plasticware. Samples were pipetted every minute for the first 10 minutes and every 5 minutes after until the solution had been prepared for 20 minutes. Data from this experiment can be found in Figure 5.

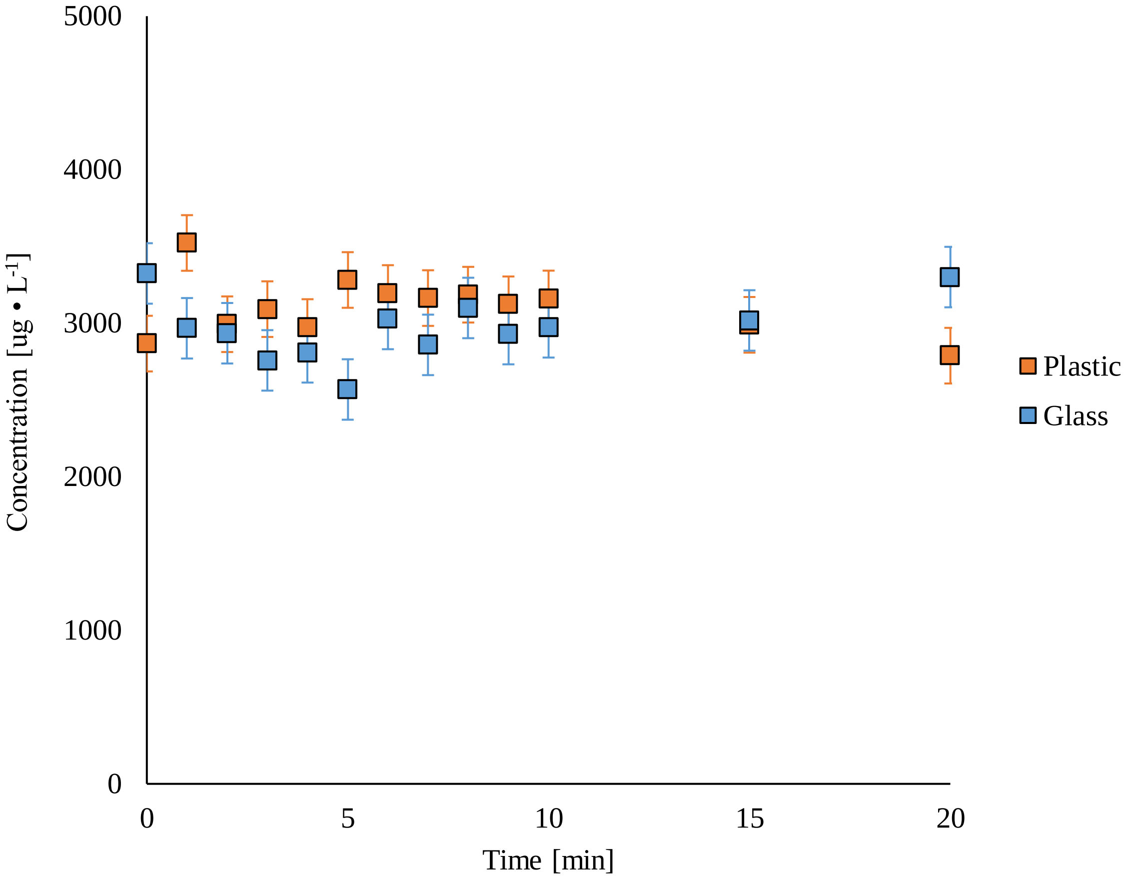

Figure 5: Concentrations of identical Nd solutions made with ultrapure water over time and prepared using volumetric flasks and storage containers constructed of different materials

Measured concentrations, based on ICP-AES, gave values between 2,569 and 3,324 µg • L^{-1} with an average of 2,967 ± 197 µg • L^{-1} for the glass bottles. The plastic bottle values ranged between 2,789 and 3,523 µg • L^{-1} with an average of 3,103 ± 181 µg • L^{-1}. Similar to the last experiment, 76.9% of the glass bottle samples showed lower concentrations than plastic bottles, but only 7.6% with statistical significance, and the average concentration of plastic bottles were higher. Based on these results, along with the previous experiment, only plastic materials were used in solution preparation and experimentation. The rationale was that each transfer of the solution to different glassware could compound the effect further while plasticware may minimize the effect. The concentration in all experiments to follow may be affected by the downward trend apparent in the plastic bottles. There were differences between the desired concentration and the initial measured concentration depending on the duration the stock solutions and prepared solutions aged. Time and equipment limitations prevented testing the concentration of the stock solutions over a long period of time to confirm this hypothesis.

Water Production Optimal Dose

The goal of this experiment was to determine the optimal dose and time of contact for activated carbon to treat a 3,000 μg • L^{-1} REE solutions. An optimal dose was defined here as the amount of activated carbon needed to moderately reduce the amount of REE in solution without being in surplus. This way, the time it takes to reach the adsorption capacity of the activated carbon can be determined when adsorption of REEs ceases.

CAC was initially added at a dosage of 50 mg • L^{-1} to 3,000 μg • L^{-1} REE solutions (or an REE loading of 60 mg of REE per gram of activated carbon). A plot of the data can be seen in Figure 6.

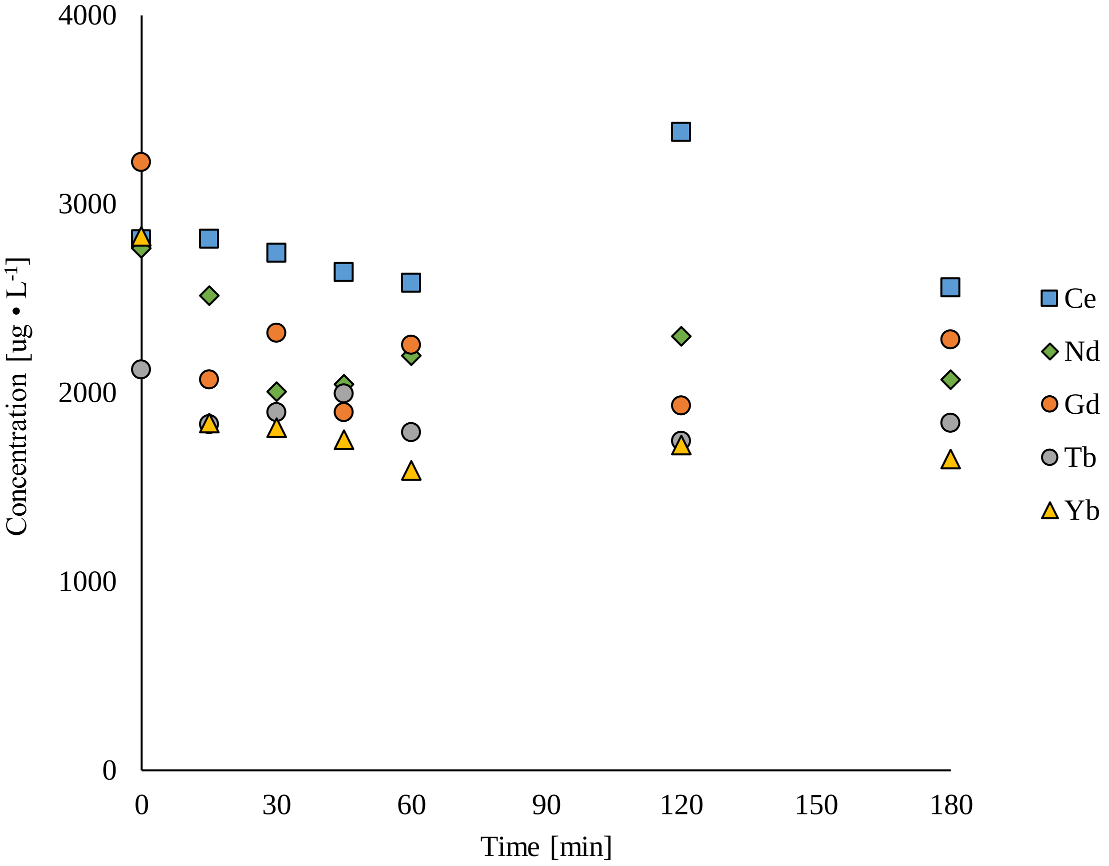

Figure 6: Concentrations of REE solutions made with ultrapure water over time using 50 mg • L^{-1} of CAC

It was found that Yb, the heaviest of the REEs tested, had the highest maximum concentration reduction of 43.8%. Likewise, Ce, the lightest of the REEs tested, had the lowest maximum concentration reduction of 9.0%. It is important to note the unusual jump in concentration of Ce after 120 minutes, but this was disregarded as an outlier. The full list of maximum concentration reductions can be seen in Table 3. There was not enough adsorption for any tested REE to justify this dose of activated carbon as the optimal dose. The overall trend in the data shows that as the REEs increase in atomic weight, the concentration was lower, and therefore adsorption was higher.

Table 3: Maximum reductions in concentration from Figure 6

Element	Maximum Reduction (%)
Ce	9.0
Nd	27.5
Gd	41.1
Tb	17.9
Yb	43.8

The dose was subsequently increased to 2,500 mg • L^{-1}, which resulted in nearly 100% adsorption of REEs onto the activated carbon within 15 minutes. The dose was reduced to 500 mg • L^{-1} but also resulted in 99.99% removal of all REEs after 15 minutes, although there were slightly higher final concentrations than the 2,500 mg • L^{-1} dose. In both cases, each tested REE is removed in the first few minutes, showing an oversaturation of activated carbon. A plot of the concentrations over time with a 500 mg • L^{-1} dose can be seen in Figure 7.

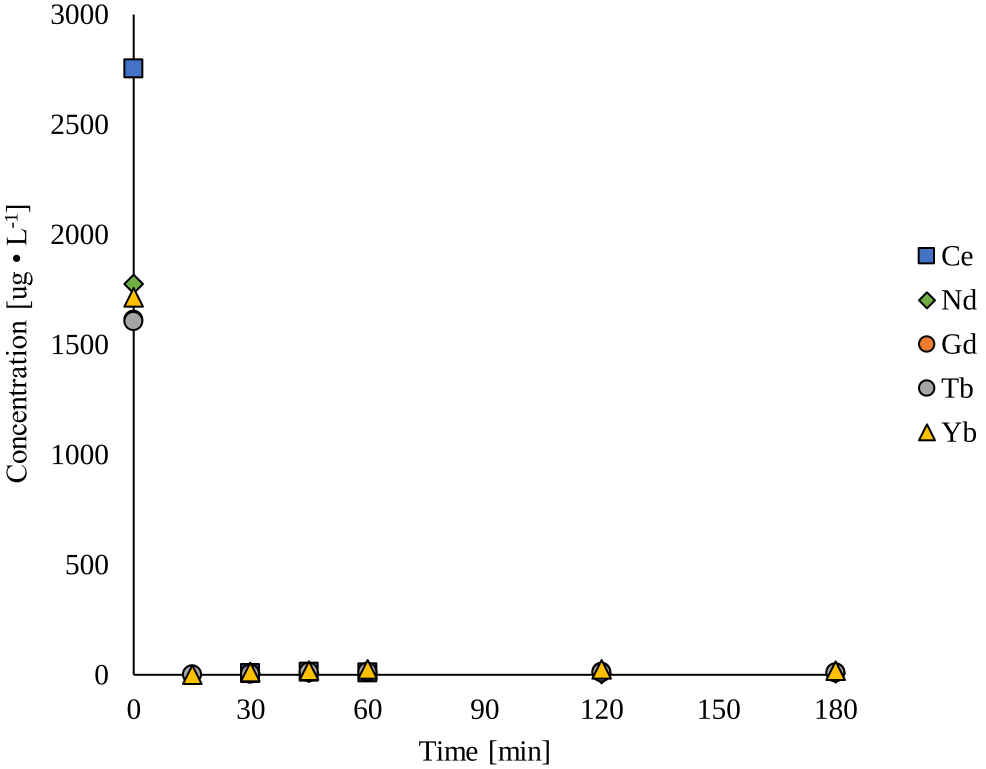

Figure 7: Concentrations of REE solutions made with ultrapure water over time using 500 mg • L^{-1} of CAC

From these experiments, it was determined that the optimal dose of activated carbon must be between 50 mg • L^{-1} and 500 mg • L^{-1}. In this range, the activated carbon must reach its adsorption capacity while also removing only a moderate amount of all REEs.

It was decided to test Ce as a representative REE for a period of 120 minutes using CAC doses of 75, 125, 250, and 375 mg • L^{-1} to determine the optimal dose within the 50 - 500 mg • L^{-1} range. Ce concentration over time at increments of CAC doses can be seen in Figure 8.

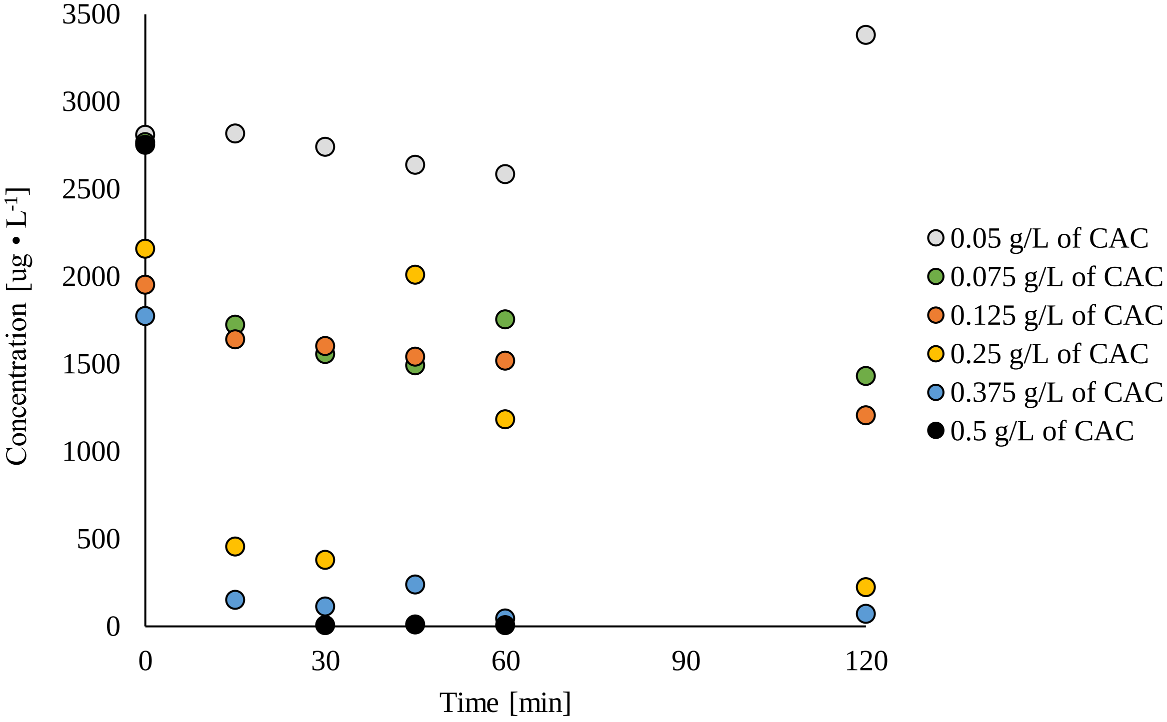

Figure 8: Concentrations of Ce solutions made with ultrapure water over time using varying doses of CAC

The optimal dose was determined to be 125 mg • L^{-1}. At higher doses, too much Ce is adsorbed to claim the activated carbon reached its adsorption capacity. At lower doses, such as 50 mg • L^{-1}, there is almost no change in concentration and therefore the adsorption capacity cannot be determined. This dose poses the same outlier as noted previously. Uncertainty in the data was taken into consideration when deciding the optimal dose. Fluctuations in initial concentrations may be a result of inaccurate readings from the ICP-AES or from adsorption to the bottle as previously mentioned. This can also be attributed to the fluctuations seen in the 250 mg • L^{-1} dose where the concentration suddenly spikes at 45 and 60 minutes, despite similarities between the concentrations at 30 and 120 minutes. The optimal dose of 125 mg • L^{-1} of activated carbon was used for the remaining water production experiments.

Effects of Activated Carbon on REEs

For the first experiment, CAC was added at 125 mg • L^{-1} to 3,000 µg • L^{-1} REE solutions made with ultrapure water and sampled across 120 minutes. Each REE was tested individually to identify the effect on each element. The results from this experiment can be found in Figure 9.

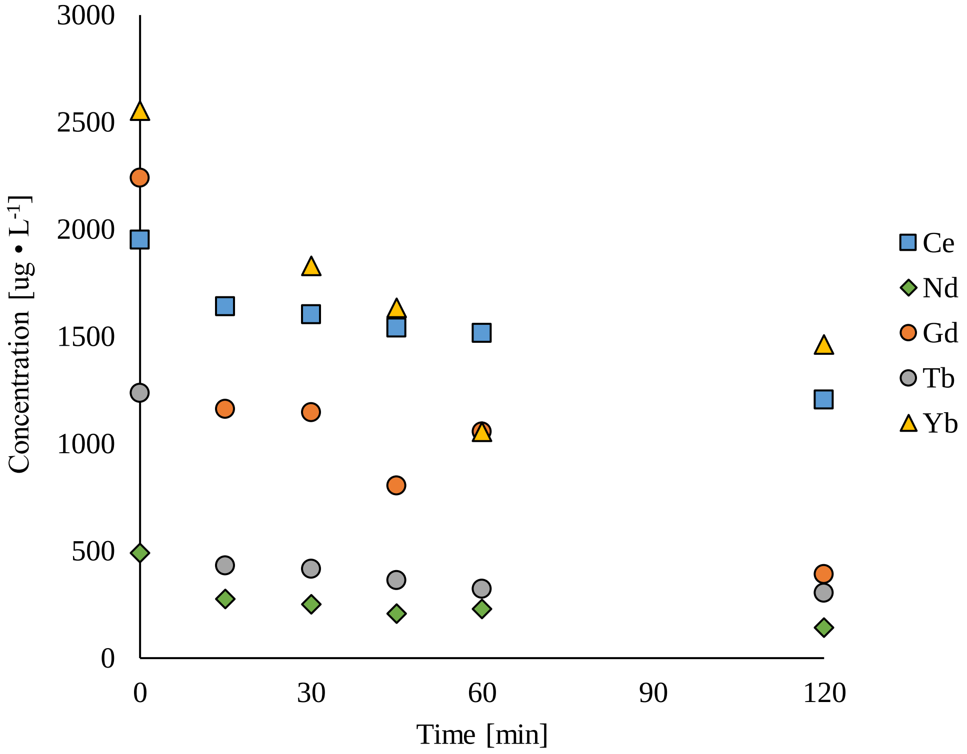

Figure 9: Concentrations of REE solutions made with ultrapure water over time using 125 mg • L^{-1} of CAC

For all five REEs, there was an excess of REE in the solution, so the activated carbon reached its adsorption capacity before all of the REEs were adsorbed. Satisfying this criterion allows the data to be used in adsorption capacity calculations, which are discussed in Characterization of Activated Carbon section of this report. An unexpected result was found where Yb, the heaviest of the REEs, decreased in concentration by 58.69% and ended with the highest concentration remaining in the solution while Nd, the second lightest REE, decreased in concentration by 70.54% and ended with the lowest concentration. It was expected that Yb would adsorb the most and follow the same trend where adsorption increases with the atomic weight as seen in previous experiments and in experiments that will be discussed later. Nd started at an unusually low initial concentration which allowed it to be the lowest concentration among all of the REEs over time. Even if it started at this low concentration, we would have expected all of the Nd to be adsorbed at this dose. We are unsure of what else may have caused this trend in the data. However, Ce, Gd, and Tb follow the expected trend where the adsorption increases with the atomic weight of the REE.

Following these experiments with CAC, the biologically produced banana and orange activated carbon samples were tested as feasible adsorbents for REE removal in water production. BPAC was produced in abundance, allowing for experimentation at the optimal dose for each individual REE. The results of these experiments can be seen in Figure 10.

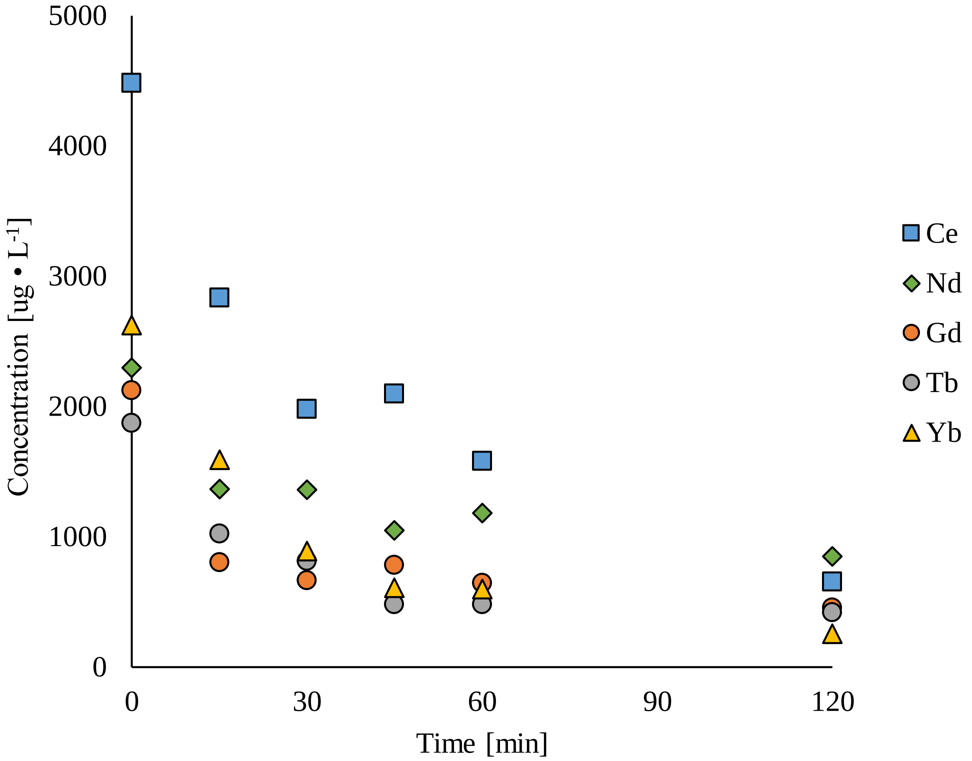

Figure 10: Concentrations of REE solutions made with ultrapure water over time using 125 mg • L^{-1} of BPAC

In all tested elements, there is a clear decrease in concentration of REE over the 120 minute sampling period. Yb showed the highest decrease in concentration at 90.2%, which is a consistent trend for the heaviest REE tested. Nd, the second lightest element tested, resulted in the lowest adsorption, with a decrease in concentration of 63.0%. Ce showed a concentration decrease of 82.0%, however the unusually high initial concentration of 4,488 µg • L^{-1} plays a major role in this decrease. It appeared that Ce did not reach its adsorption capacity because of a continuous decrease in concentration from 60 to 120 minutes, but all other REEs showed a minor change during this time. This may be due to uncertainty in measurements while preparing stock solutions. From this data, it is evident that BPAC is a reliable adsorbent for the removal of REEs in water production.

Next, the OPAC was analyzed for its effectiveness of REE removal. However, due to the limited supply of OPAC, only a single experiment was performed. Ce was chosen as the preferred experimental element, as it was the most extensively tested REE to this point and its behavior under activated carbon treatment was the best understood.

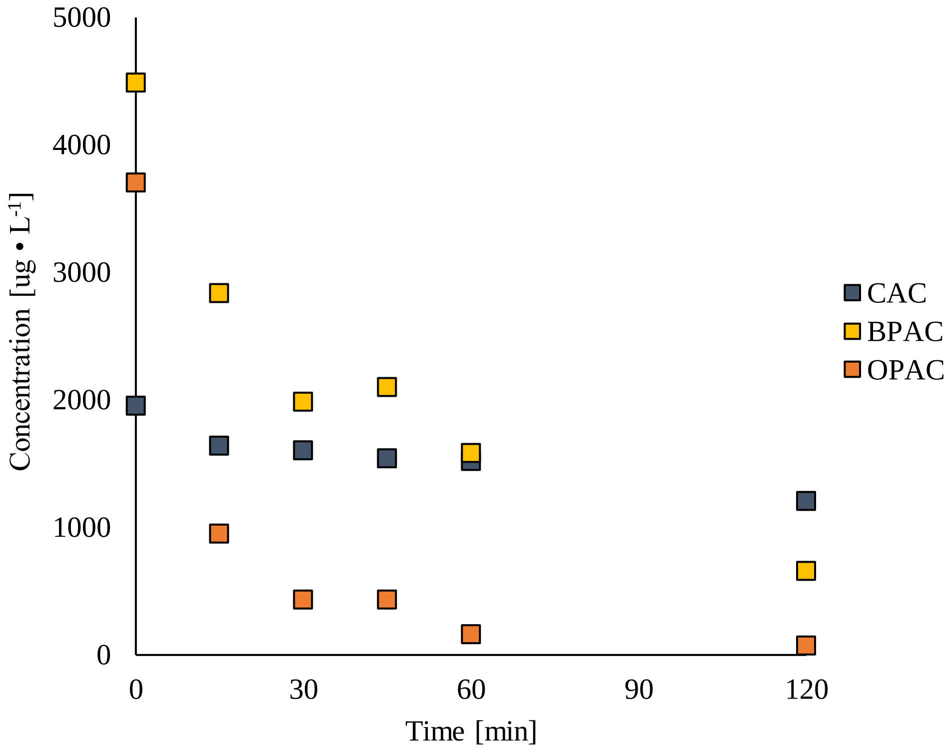

Figure 11: Concentrations of Ce solutions made with ultrapure water over time using 125 mg • L^{-1} of CAC, BPAC, and OPAC

The OPAC showed a 98.0% removal of Ce at the optimal dose of 125 mg • L^{-1}, compared to 85.3% for BPAC, and 38.2% for the CAC. While only performed in one experiment, it is shown that the OPAC has a high capacity for removing REEs in water production. Both biologically produced activated carbon samples performed better than the CAC sample. This could be due to higher surface area in the BACs, or a difference in pore sizes; this will be explained in further detail in the Characterization of

Activated Carbon section. Based on previous results, it is expected that further experiments with OPAC would show equally, if not higher, adsorption of the heavier REEs.

Adsorption Selectivity of REEs

Selectivity in adsorption between LREEs and HREEs in ultrapure deionized water was the next tested parameter. Three REEs were selected ranging from LREE to HREE to determine if certain REEs are preferentially adsorbed. A 3,000 μg • L^{-1} REE solution was made by adding 1,000 μg • L^{-1} of each REE. The REEs used were Ce (LREE), Yb (HREE), and Gd as the third with an approximately average molecular weight of the LREE and HREE. The selectivity was determined by assessing if one element's concentration was lower than the others when the adsorption capacity was reached. Data from this experiment using CAC can be seen below in Figure 12.

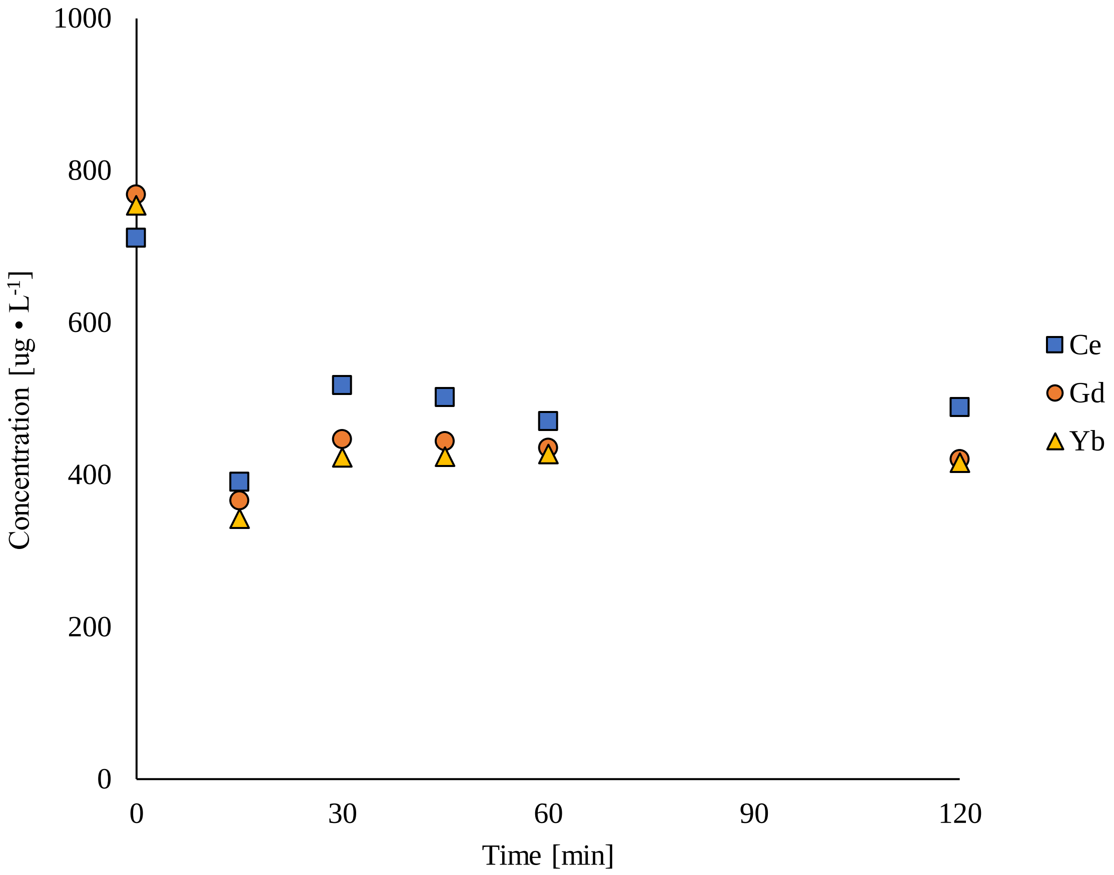

Figure 12: Concentration of mixed REE solutions made with ultrapure water over time using 125 mg• L^{-1} of CAC

The largest decline in concentration for all REEs occurred at the 15 minute sampling period, however an overall negative trend continued throughout the 120 minute experimental period. The Yb concentration decreased more substantially than both the Gd and Ce. After the 120 minute experiment, Yb concentrations decreased 48%. The Ce concentration, by contrast, showed the lowest decrease in concentration, at 31%. Gd, as expected, was adsorbed at a rate between the LREE and HREE, with a decrease in concentration of 45% over the course of experimentation. From this, we can conclude that REEs with higher atomic weights adsorb onto activated carbon more favorably than their lighter counterparts.

A similar experiment was run to determine if there was selectivity in adsorption of various REEs in river water. In these experiments, anions and cations in the river water could compete for adsorption to the activated carbon and change the selectivity of the REEs in the previous experiment. The full composition of the Moselle River water can be found in Appendix B Table B.22. Experiments were run using the optimal dose of CAC and BPAC in 1,000 μg • L^{-1} Ce, Gd, and Yb solutions made with river water. The data from this experiment can be found in Figure 13.

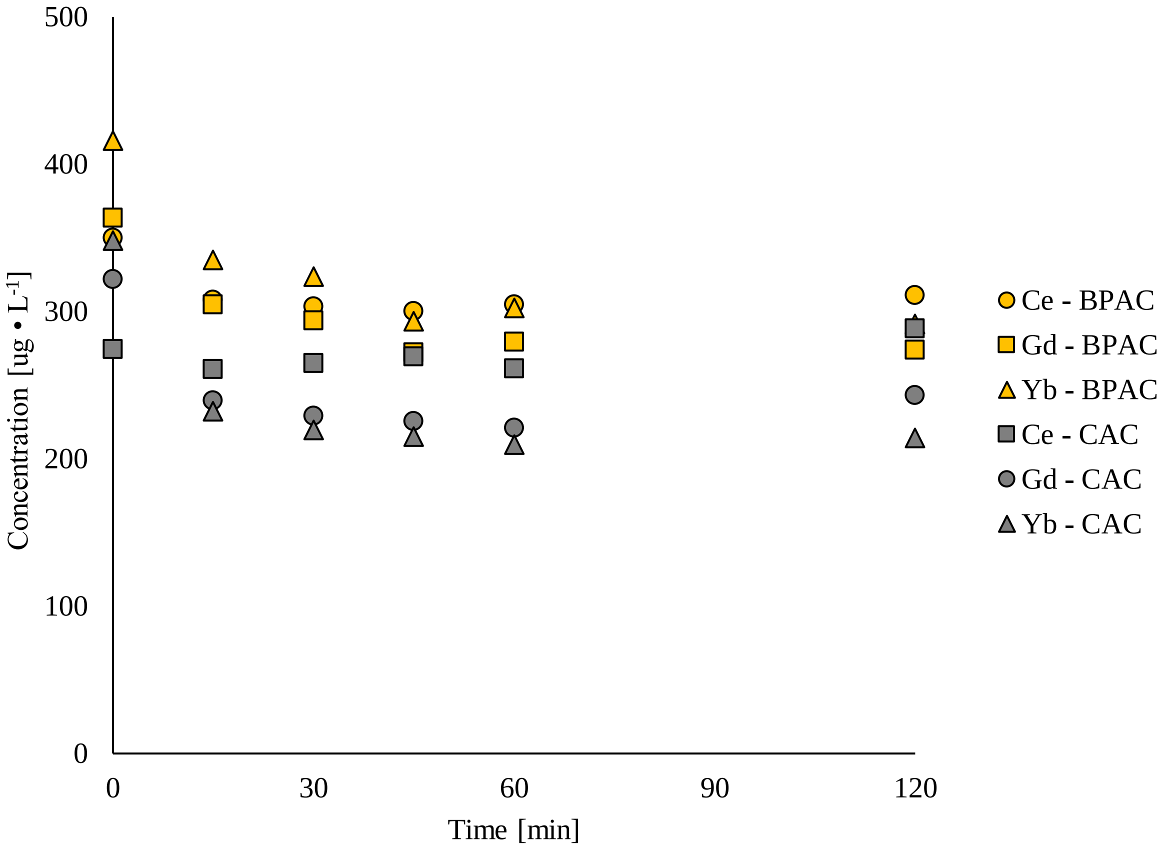

Figure 13: Concentration of mixed REE solutions made with river water over time using 125 mg • L^{-1} of CAC and BPAC

From this experiment, a clear distinction is made between the ultrapure and river water solutions. In the mixed REE experiment using ultrapure water performed with CAC, percent reductions in REE concentrations are significantly higher than with this river water experiment. For example, the Gd concentration was reduced 45% when in ultrapure water, while it was only reduced 24.5% while mixed with river water. From this, it can be concluded that the other constituents in the river water have a significant impact on the removal of REEs using activated carbon. Elements such as sodium, potassium, and calcium are prevalent in the river water, possibly adsorbing to the activated carbon more favorably than the REEs.

In addition, the BPAC removed a higher percentage of Ce and Gd than the CAC, but the final concentrations appear higher for BPAC due to higher initial concentrations. This is consistent with our previous BPAC experiments, reinforcing the effectiveness of the biologically produced activated carbon samples.

Another notable result from this experiment is the overall increase in Ce concentration across the 120 minute duration for the CAC. The low initial concentration could play a role in this result, as the dose of Ce in solution was 1,000 $\mu g \bullet L^{-1}$. In addition, all other concentrations prior to the 120 minute sample are lower than the initial concentration, with a spike at the 120 minute mark. This could potentially be attributed to an error in the ICP-MS readings.

Effects of Banana Peel Biochar on REEs

Banana peel biochar produced by Dr. Le Brech was tested under similar experimental conditions to observe its effectiveness in REE removal. Three mixed REEs (Ce, Gd, and Yb) were added to ultrapure water in 1,000 $\mu g \bullet L^{-1}$ doses, with 125 $mg \bullet L^{-1}$ of the banana biochar added at the beginning of testing. Figure 14 represents the results gathered from this experiment.

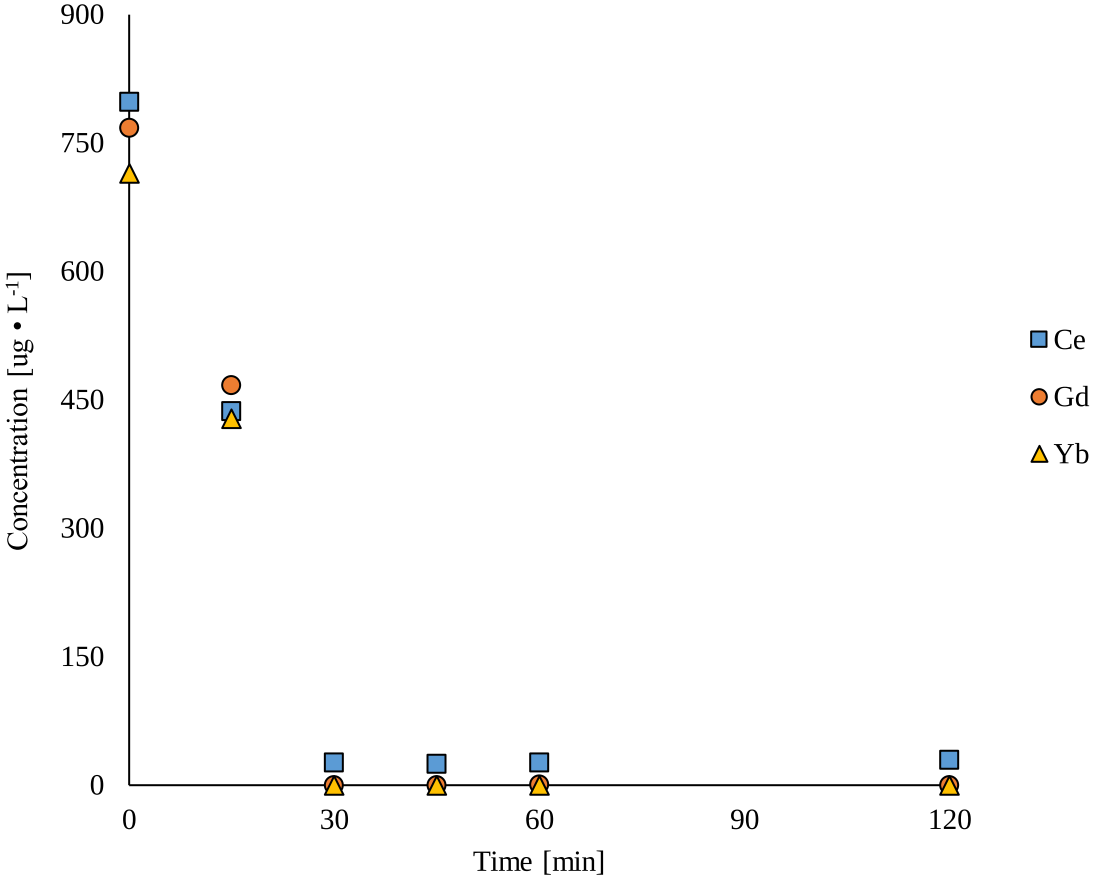

Figure 14: Concentration of mixed REE solutions made with ultrapure water over time using 125 mg• L^{-1} of banana peel biochar

As seen in the figure above, the banana biochar works much faster than the activated carbon samples, removing 98.9% of REEs within 30 minutes of addition. The banana biochar is produced with a slightly different procedure than the BAC samples, which may develop a higher surface area or larger pores that result in faster adsorption. In addition, this experiment demonstrates a similar pattern as seen throughout these results. The LREE, Ce, did not adsorb as completely as the medium or heavy weight REEs in solution. As mentioned, this could be a result of the weight of the REE, being a smaller element it may not adhere as easily to the available pores in the biochar. Banana biochar does prove to be an effective adsorbent for REEs in water treatment, with very quick results. However, further experimentation is recommended to verify these results.

Characterization of Activated Carbon and Biochar

The data from Figure 9, Figure 10, and Figure 11 were used to calculate the adsorption capacity for CAC, BPAC, and OPAC, respectively, using equation 1. The adsorption capacity results are summarized in Figure 15.

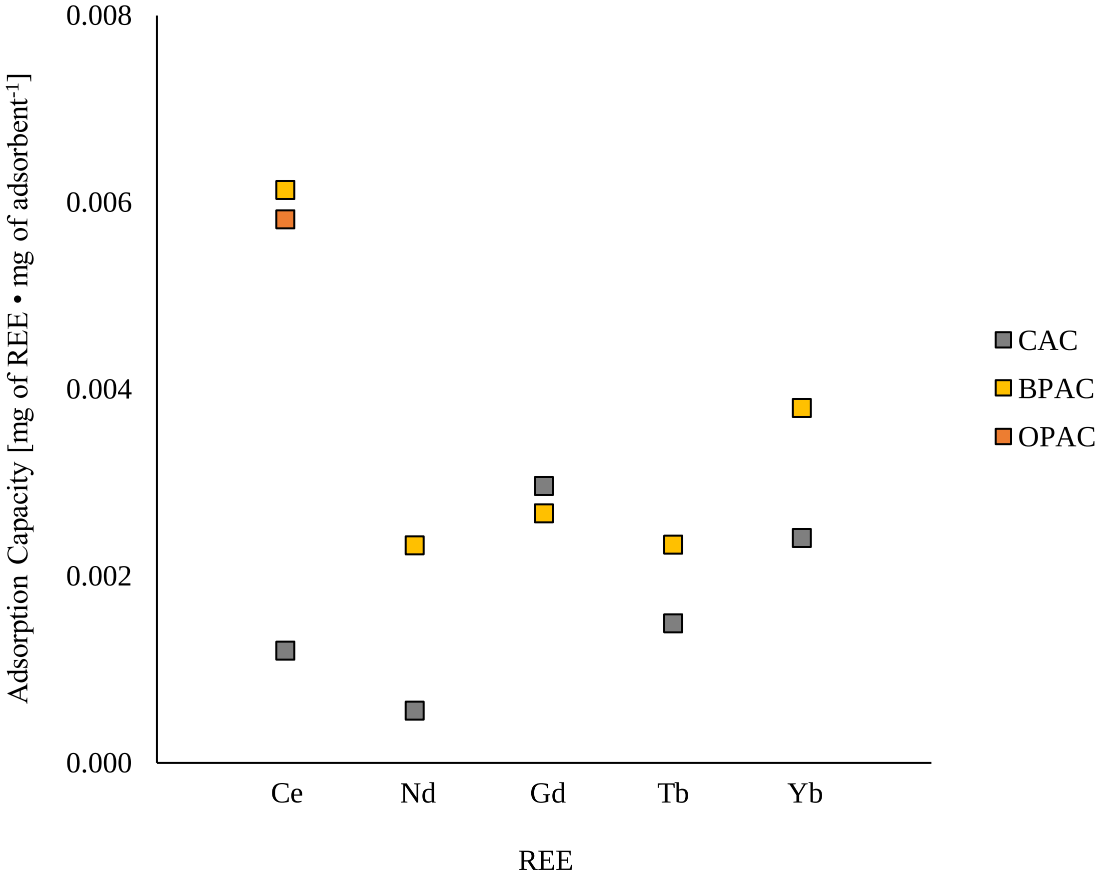

Figure 15: Adsorption capacities of REEs for commercial, banana peel, and orange peel activated carbon

Overall, the BPAC shows the highest adsorption capacity across 4 out of 5 of the tested REEs. A higher adsorption capacity means that less carbon is required to reduce the concentration of REE. In a water treatment facility, the BPAC would be favorable, as less carbon would need to be added for sufficient removal of REE. However, the OPAC also shows a very high adsorption capacity for Ce, the only REE tested with this activated carbon. Further experimentation is required to determine if the OPAC would perform equally well with other REEs. The BPAC, as a result of current available data, can be identified as the most effective activated carbon for REE removal in water production. The banana peel biochar adsorption capacity was not included because nearly 100% of the REEs were removed. The optimal dose for activated carbon is not the optimal dose for the banana peel biochar.

No trend between the weights of the REE compared to the adsorption capacity can be identified. This could be a result of the pore size and surface area of each activated carbon sample being sufficient to adsorb even the heavy REEs tested. Another potential explanation can be related to the initial concentrations of REEs. The high variation in starting concentration can alter this finding. Further experimentation is required with controlled initial concentrations to determine if this lack of trend remains consistent.

An SEM was used to analyze the pore size and distribution on the activated carbons. For the BPAC, images were taken at each preparation step to observe how the activated carbon progressed to its final form. For the CAC, OPAC, and banana peel biochar, images of just the final product were obtained. Figure 16 shows SEM images of BPAC in the steps leading up to make activated carbon.

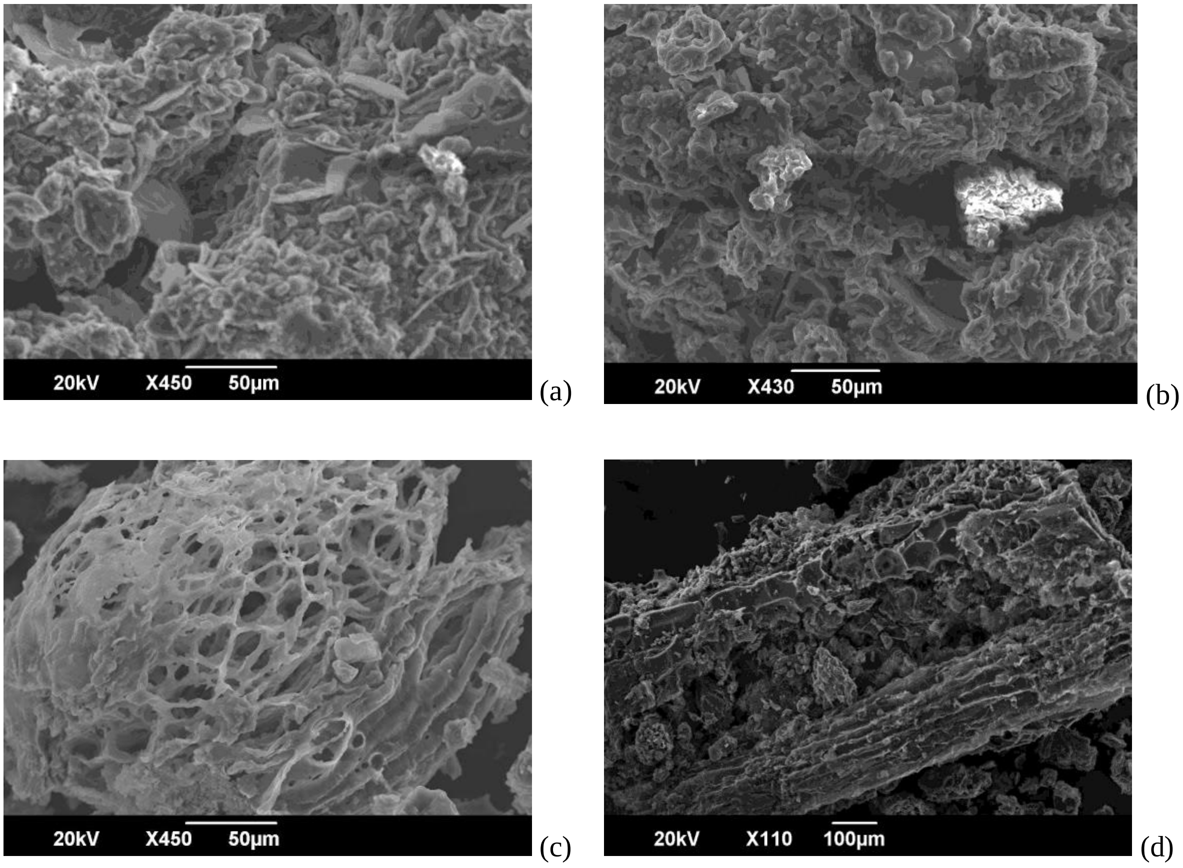

Figure 16: Banana peel activated carbon under SEM. (a) Banana powder after being dried and pulverized, (b) Banana powder after carbonization at 400°C, (c) Banana powder after going through 45% NaOH bath and dried at 105°C, (d) Banana peel activated carbon sample

From Figure 16, it is evident that a larger surface area develops on the structure of the BPAC. A higher concentration of pores becomes prominent as the steps progress. For comparison, SEM images of finished CAC, OPAC, and banana peel biochar can be found in Figure 17, Figure 18, and Figure 19, respectively.

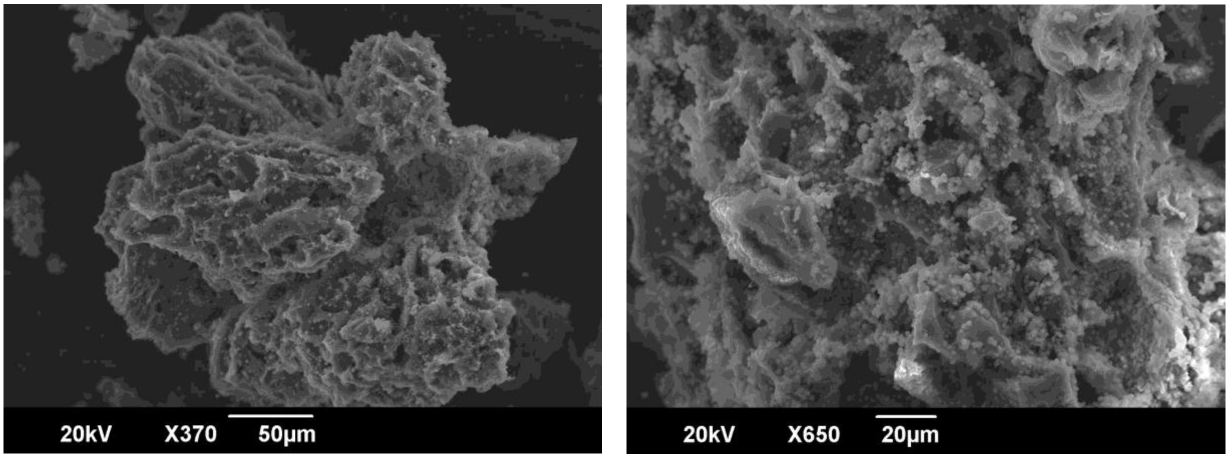

Figure 17: SEM images of finished orange peel activated carbon samples

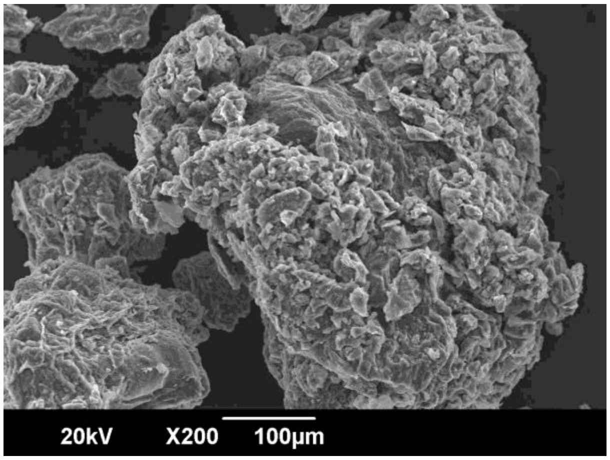

Figure 18: SEM images of finished banana peel biochar samples

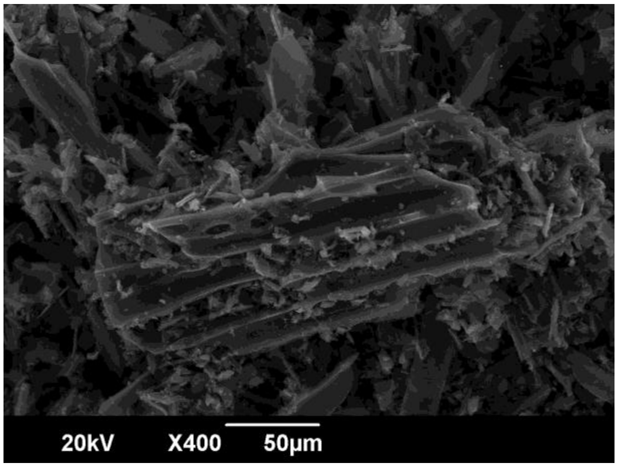

Figure 19: SEM images of finished commercial activated carbon samples

The pore size of BPAC and OPAC is relatively large compared to CAC. The CAC showed fewer pores and more of a crystalline structure with flatter surfaces. The OPAC had a unique characteristic where small beads were scattered across the structure. Both characteristics can be attributed to a high surface area, and therefore high adsorption capacity. The structure of the banana peel biochar had few similarities with the activated carbon samples. It appeared to be a solid mass with a lower surface. This was expected because it does not undergo the same procedure as activated carbon to increase the surface area. The banana peel biochar, however, outperformed all activated carbon samples by completing removing REEs from a solution at the optimal dose of 125 mg • L^{-1}, suggesting that the surface area may be larger or that there is another mechanism that promotes adsorption. A BET analysis is recommended in a later study to analyze the specific surface areas of each sample.

In addition to the SEM analysis performed on each sample, EDX analysis provided quantitative elemental identification to give insight to the composition of CAC and BPAC samples. Notable atomic percentages of elements for CAC and BPAC are outlined in Table 4. EDX analyses of OPAC and banana peel biochar were not completed due to equipment complications.

Table 4: Atomic percentages of various elements in commercial and banana peel activated carbon

Element	Commercial (%)	Banana (%)
Na	10.72	36.98
Al	6.65	4.98
Si	5.84	5.01
P	5.34	4.95
S	7.09	0.00
K	5.52	5.33
Ca	5.27	5.30
Fe	7.27	4.94
Ni	9.85	6.75
Cu	12.17	8.30
Zn	15.25	10.36
As	6.41	5.46
Pb	2.61	1.65

From the EDX Analysis, it is seen that the BPAC is composed of a much higher atomic percentage of sodium than the CAC, at 36.98% and 10.72%. In addition, another notable change can be seen in the sulphur content of the activated carbon samples. The BPAC has no sulphur content, while the CAC is composed of 7.09% sulphur on the atomic level. Aside from these notable differences, the compositions of the activated carbons are relatively similar.

While still not a researched topic, these small changes in composition could be responsible for the immense changes in REE adsorption, as seen in the Effect of Activated Carbon on REEs section of the results.

Wastewater Treatment Results

The synthetic wastewater composition was analyzed using an ICP-AES. This was done prior to wastewater testing to ensure the accuracy of the synthetic wastewater. The accuracy of the wastewater was based off influent wastewater samples from the Grand Nancy WWTP. The original synthetic solution was a stock solution 20 times the strength of the desired composition, to allow for multiple experiments to be conducted. Upon analysis, the full elemental composition, which can be found in Appendix B Tables B.15-B.21, matched the composition of the actual wastewater aside from the Ca concentrations, which were significantly lower. One potential reason for this difference could be the strength of the stock, being so densely packed the Ca had precipitated out of solution. As a result, an additional stock solution was prepared at five times strength, to allow for less precipitation to occur. Both stocks were used in experimentation for comparison. The entire results of these compositions can be found in Appendix C Table C.2.

Dose of $FeCl_3$ was the first analyzed parameter: for 0, 1, 2, 3, 4, and 5 mg • L^{-1}, with an initial Gd concentration of 3000 μg • L^{-1}. Initially, the $FeCl_3$ was added as a solid, resulting in the 0 and 1 mg • L^{-1} jars creating large clumpy flocs that formed at the base of the jar. The higher doses of $FeCl_3$ created more abundant flocs that were smaller in size and spread more evenly throughout the jars. In later tests, the $FeCl_3$ was added as a liquid solution, to allow for more efficient distribution of $FeCl_3$ to the solution. Figure 20 depicts the experimental setup, as well as the jar dosed at 2 mg • L^{-1} during the rapid mix, flocculation, and settling stages.

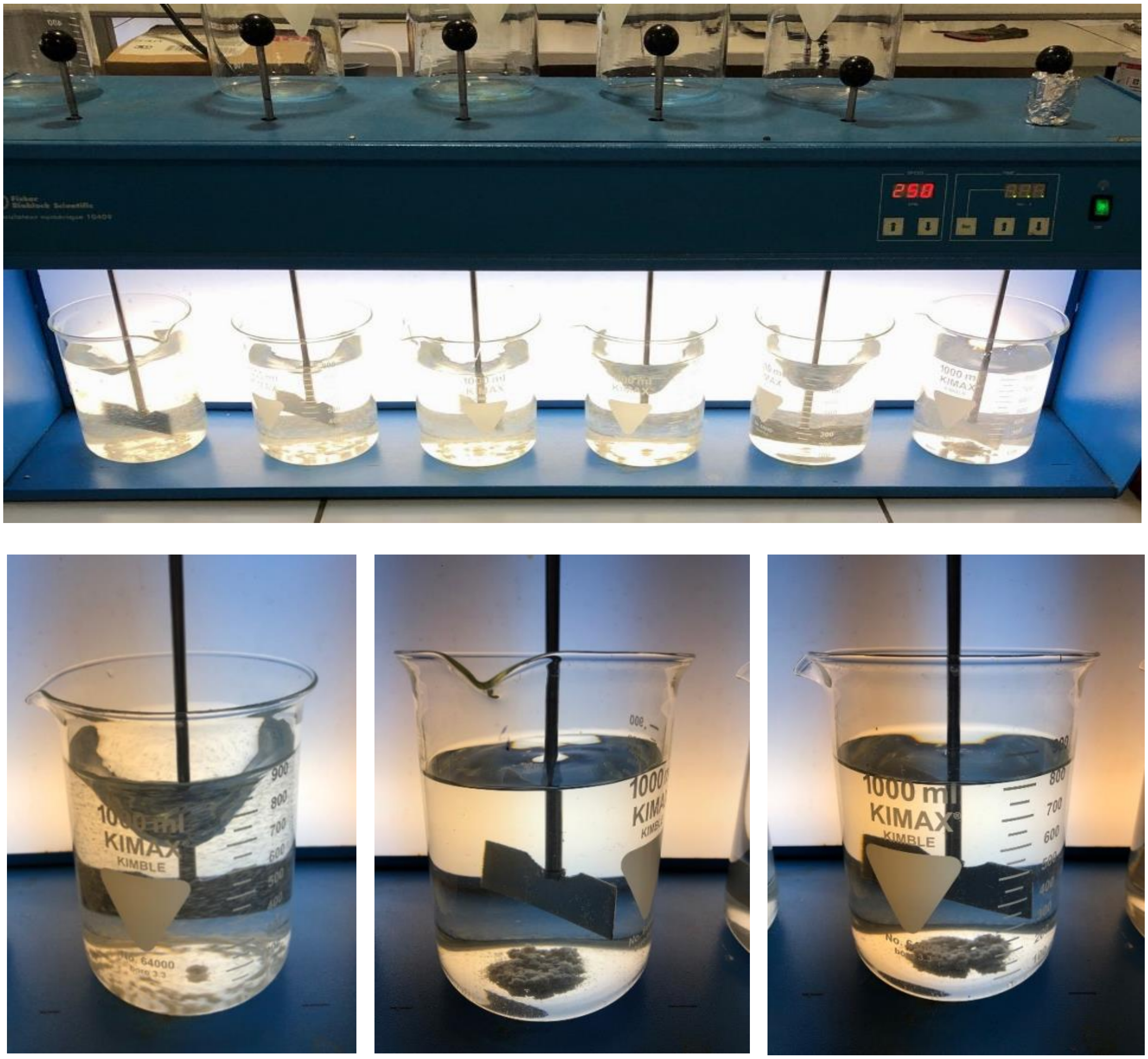

Figure 20: (a) Jar testing experimental set-up; (b) 2 mg • L^{-1} $FeCl_3$ during rapid mix period; (c) 2 mg • L^{-1} $FeCl_3$ during flocculation period; (d) 2 mg • L^{-1} $FeCl_3$ during settling period

Testing ensued for both the original 20 times strength stock solution as well as the five times strength stock. This was done to see the effect of the Ca on the settling process. The results of these experiments can be seen in Figure 21.

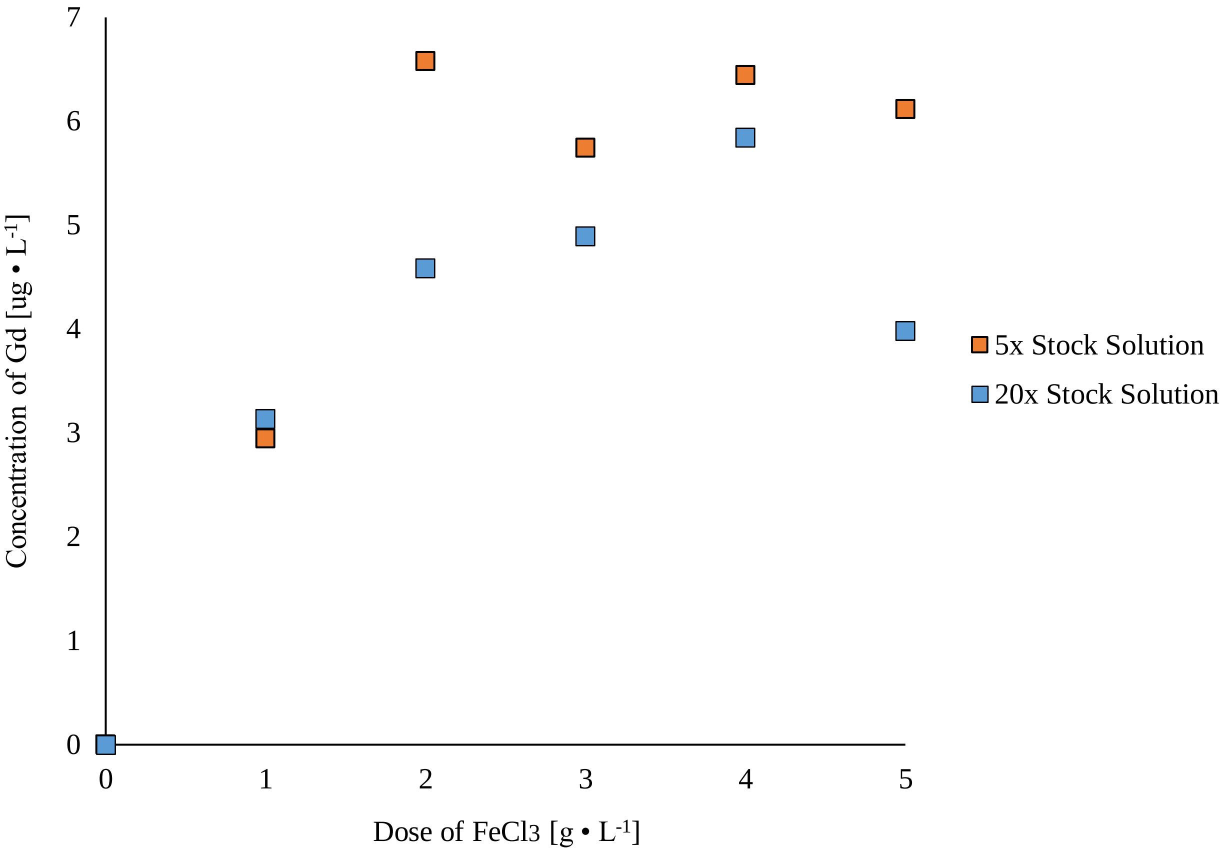

Figure 21: Concentration of gadolinium versus dose of $FeCl_3$ using two types of stock solution

As seen from the figures above, there is no trend between the dose of $FeCl_3$ and the amount of Gd removed from solution. The concentration of Gd reaches 0 µg • L^{-1} in the absence of $FeCl_3$, and remains nearly 0 µg • L^{-1} as the dose is increased. In addition, the varying stock solutions had little effect on the results, with Gd concentrations in solution never exceeding 7 µg • L^{-1}. A possible cause of these results could come from the wastewater treatment process. The coagulation, flocculation, and settling periods could be sufficient for the removal of Gd, regardless of the dose of coagulant. It is possible that the Floerger® AN 923 VHM solution and fine sand were able to bind to the Gd and settle it out of solution, as these components were constant across each sample. Phosphate presence can also be attributed to this result, as it is proven to precipitate REEs out of solution.

The above experiment was repeated with unfiltered secondary treatment effluent wastewater from the Grand Nancy WWTP, under two conditions. The first condition was with an additional 3000 μg • L^{-1} Gd added to solution, and the second was with a mixture of REEs, mimicked from the water production experiments. Similar results were obtained from these experiments, showing the complete removal of REEs regardless of the presence of $FeCl_3$. Again, this could be a result of the other components added to solution to aid in the coagulation process. From previous research, it was determined that phosphates present in wastewater precipitate REEs out of solution. As this wastewater, including the synthetic wastewater, both had phosphates present; it is likely that the REEs precipitated out of solution by aid of the phosphate, and not the $FeCl_3$. In addition, filtration through a 0.45 μm filter was required for each sample to not damage the analytical equipment. It is possible that some REEs were filtered out of the final samples. The full results of these experiments can be found in Appendix B Tables B.11-B.14.

Conclusion

Global demand for REEs is increasing at an exceptional rate, with no anticipated decrease in future development. With this increase manufacturing demand, there is anticipated growth of REE contamination in water bodies and the Rhine River of Europe. And while still not well-documented, there are proposed health concerns of ingesting REEs. We sought to determine optimal means of removing these REEs in water production and wastewater treatment, to provide safe drinking water for those in the Rhine River watershed, as well as safe water to be used by the ecosystem.

In water production, activated carbon is the most common adsorbent used to remove contaminants by physical means. Activated carbon, with high surface area and pore volume, is ideal for which contaminants to adhere. We tested activated carbon in varying doses to different REEs and REE mixtures to determine the effect of removal. Aside from commercially produced activated carbon, we developed two biological activated carbon samples: one from banana peels (BPAC), the other from orange peels (OPAC).

An optimal dose of 125 mg • L-1 of activated carbon for a solution containing 3,000 µg • L-1, or a loading corresponding to 24 mg of REE per gram of activated carbon was identified; where REE removal was moderate, without being present in surplus. BPAC and OPAC both proved to be effective means of removing REEs in water production; with a higher removal rates and higher adsorption capacities than the commercially produced activated carbon. When mixing three REEs in solution together and repeating the experiment, it was found that the heavier REEs tend to be more easily adsorbed to the activated carbon than its lighter counterparts. Jar testing was performed to mimic the wastewater treatment process for further testing. $FeCl_3$ was tested at five different doses to identify the optimal dose to remove REEs without being in excess. From these experiments, no dose of $FeCl_3$ proved to be more effective than any other, when tested with synthetic or actual wastewater. There was a near 100% removal of REEs when tested with Gd individually or with Ce, Gd, and Yb mixed in solution. From this, we concluded the effectiveness of coagulation, flocculation, and sedimentation for the removal of REEs using only fine sand and Floerger® AN 923 VHM solution. This result is independent of weight of REE, as proven through the mixed REE experiment.

With an overwhelming number of uses in various fields of development, it is no surprise that the uses of REEs are growing at their current rate. With this growing use, it is imperative to move forward with caution, as health risks to humans and the environment are still not well-documented. We pursued means of removing these elements from water supplies, with positive results for both water production and wastewater treatment. While further testing is still required to develop this research to completion, this project demonstrates promise for the removal of REEs by the means outlined in this report.

Recommendations

Moving forward, the next immediate steps are to finish experiments using OPAC. First, additional activated carbon from orange peels must be prepared. Then, the activated carbon must be tested at the optimal dose of 125 mg • L^{-1} with four individual REEs at 3,000 μg • L^{-1} (Nd, Gd, Tb, and Yb) as well as a test with three REEs mixed together at 1,000 μg • L^{-1} each (Ce, Gd, and Yb). Afterwards, further experiments can be conducted using the banana peel biochar method that was briefly introduced but was not assessed in depth. Orange peel biochar can also be tested. The biochar preparation is easier and faster than the activated carbon.

In preparation of BACs, we recommend pulverizing the BAC into fine particles after the final step. Our observations of the activated carbon experiments have found that CAC scatters across the solution while the BACs remain in clumps. So while successful at lowering the REE concentrations, the adsorption capacity could potentially increase with this additional step. To aid in the characterization of the activated carbon and biochar samples, BET analysis could be completed. This will give an accurate reading of the surface area of the samples, which will strengthen the characterization.

Based on the findings identified in the water production study, the future directions should focus on determining the factors that contribute to uncertain results before moving forward with experimentation. Separate investigations should be made to determine the concentration of the stock solution using more precise measurements as well as the effects on the REE concentration in the refrigerator over a long period of time. Both factors are possible explanations for the unusually low data points in our report, primarily the initial concentrations of many experiments.

In the wastewater treatment study, we suggest using a new jar testing station. The current station is equipped with six stirrers that stir at inconsistent speeds. In an experiment such as coagulation and flocculation where stir speed is essential, we highly recommend resolving this issue before experimentation continues if strong results are desired. In preparation of the synthetic wastewater solution, a stock solution with a concentration no higher than five times the concentration outlined in the formula should be prepared to avoid precipitation of elements. Finally, we recommend that an organic Gd chemical be tested in addition to the mineral salt, in both wastewater and water production testing. This test can help prevent Gd precipitation due to phosphates in the wastewater, and strictly identify the effects of $FeCl_3$ on precipitation.

List of Acronyms and Abbreviations

ABET	Adult Basic Education and Training
BAC	Biological Activated Carbon
BOD	Biochemical Oxygen Demand
BPAC	Banana Peel Activated Carbon
Ca	Calcium
CAC	Commercial Activated Carbon
Ce	Cerium
CSTR	Completely Stirred Tank Reactor
EDX	Energy Dispersive X-Ray
ENSIC	École Nationale Supérieure des Industries Chimiques
Eu	Europium
Gd	Gadolinium
HREE	Heavy Rare Earth Element
ICP-AES	Inductively Couple Atomic Emission Spectrometry
ICP-AES	Inductively Coupled Plasma Mass Spectrometry
K	Potassium
La	Lanthanum
LREE	Light Rare Earth Element
Lu	Lutetium
Mg	Magnesium
MRI	Magnetic Resonance Imaging
Na	Sodium
NaOH	Sodium Hydroxide
Nd	Neodymium
OPAC	Orange Peel Activated Carbon
Sc	Scandium
SEM	Scanning Electron Microscope

Tb	Terbium
WPI	Worcester Polytechnic Institute
WWTP	Wastewater Treatment Plant
Y	Yttrium
Yb	Ytterbium

References

Akash, B., & O'Brien, W. (1996). The production of activated carbon from a bituminous coal. *International Journal of Energy Research,20*, 913-922. doi:10.1002/(SICI)1099-114X(199610)20:103.0.CO;2-7

Amuda, O., Amoo, I., Ipinmoroti, K., & Ajayi, O. (2006). Coagulation / flocculation process in the removal of trace metals present in industrial wastewater. *Journal of Applied Sciences and Environmental Management,10*(3). doi:10.4314/jasem.v10i3.17339

Annadurai, G., Juang, R., & Lee, D. (2003). Adsorption of heavy metals from water using banana and orange peels. *Water Science and Technology,47*(1), 185-190. doi:10.2166/wst.2003.0049

Bau, M., & Dulski, P. (1996). Anthropogenic origin of positive gadolinium anomalies in river waters. *Earth and Planetary Science Letters,143*(1-4), 245-255. doi:10.1016/0012-821x(96)00127-6

Bau, M., Knappe, A., & Dulski, P. (2006). Anthropogenic gadolinium as a micropollutant in river waters in Pennsylvania and in Lake Erie, northeastern United States. *Geochemistry,66*(2), 143-152. doi:10.1016/j.chemer.2006.01.002

Calgon Carbon. (2012). *Solutions for Home Water Filtration* [Brochure]. Retrieved January 10, 2019, from https://www.calgoncarbon.com/app/uploads/HomeWaterFilter_Brochure.pdf

Carr, D., Brown, J., Bydder, G., Steiner, R., Weinmann, H., Speck, U., . . . Young, I. (1984). Gadolinium-DTPA as a contrast agent in MRI: Initial clinical experience in 20 patients. *American Journal of Roentgenology,143*(2), 215-224. doi:10.2214/ajr.143.2.215

Carroll, S. (2009). *Optimising powdered activated carbon dosing procedures for removal of natural organic matter* (Unpublished master's thesis). Cranfield University. Retrieved January 21, 2019, from https://dspace.lib.cranfield.ac.uk/bitstream/handle/1826/9478/Carroll_S_2009.pdf?sequence=1&isAllowed=y

Çeçen, F., & Aktaş, O. (2012). *Activated carbon for water and wastewater treatment: Integration of adsorption and biological treatment*. Weinheim, Germany: Wiley-VCH.

Central Drug House. (n.d.). Cerium (III) Nitrate Hexahydrate Material Safety Data Sheet. Retrieved January 21, 2019, from https://www.cdhfinechemical.com/images/product/msds/63_978015593_Cerium(III)Nitrate-CASNO-10294-41-4-MSDS.pdf

Central Drug House. (n.d.). Gadolinium (III) Nitrate Material Safety Data Sheet. Retrieved January 21, 2019, from https://www.cdhfinechemical.com/images/product/msds/71_1462861073_GADOLINIUM(III)NITRATECASNO94219-55-3MSDS.pdf

Central Drug House. (n.d.). Neodymium (III) Nitrate Material Safety Data Sheet. Retrieved January 21, 2019, from https://www.cdhfinechemical.com/images/product/msds/86_913250129_NEODYMIUM(III)NITRATE-CASNO16454-60-7MSDS.pdf

Central Drug House. (n.d.). Sodium Hydroxide Material Safety Data Sheet. Retrieved January 14, 2019, from https://www.cdhfinechemical.com/images/product/msds/101_1948435969_SodiumHydroxide-CASNO-1310-73-2-MSDS.pdf

Central Drug House. (n.d.). Terbium (III) Chloride Hexahydrate Material Safety Data Sheet. Retrieved January 21, 2019, from https://www.cdhfinechemical.com/images/product/msds/106_865620713_TERBIUMCHLORIDECASNO13798-24-8MSDS.pdf

Central Drug House. (n.d.). Ytterbium Chloride Material Safety Data Sheet. Retrieved January 14, 2019, from https://www.cdhfinechemical.com/images/product/msds/114_224555490_YTTRIUMCHLORIDECASNO10025-94-2MSDS.pdf

DeVries, R. (2011). *Ferric Chloride in Wastewater Treatment* (Unpublished master's thesis). Carthage College. Retrieved January 15, 2019, from https://pdfs.semanticscholar.org/9ac8/0a8cee858ff826d0b7856383e57061e3abda.pdf

Drinking Water. (2018, January 2). Retrieved January 9, 2019, from http://ec.europa.eu/environment/water/water-drink/index_en.html

Dvorak, B., & Skipton, S. (2013, November). *Drinking Water Treatment: Activated Carbon Filtration*(Rep. No. G1489). Retrieved January 9, 2019, from University of Nebraska-Lincoln website: http://extensionpublications.unl.edu/assets/pdf/g1489.pdf

Ferris, N., & Goergen, S. (2017, July 26). Gadolinium Contrast Medium (MRI Contrast agents). Retrieved February 18, 2019, from https://www.insideradiology.com.au/gadolinium-contrast-medium/

Frijters, I. D., & Leentvaar, J. (2003). *Rhine Case Study* (Rep.). United Nations Educational, Scientific and Cultural Organization (UNESCO). Retrieved from https://unesdoc.unesco.org/ark:/48223/pf0000133303.

Gabor, A., Davidescu, C. M., Negrea, A., Ciopec, M., Grozav, I., Negrea, P., & Duteanu, N. (2017). Optimizing the lanthanum adsorption process onto chemically modified biomaterials using factorial and response surface design. *Journal of Environmental Management*,*204*, 839-844. doi:10.1016/j.jenvman.2017.01.046

Geological Survey of Queensland. (2014). Light Rare Earth Elements (LREE) opportunities in Queensland. Retrieved February 27, 2019, from https://www.dnrm.qld.gov.au/__data/assets/pdf_file/0009/306855/lree.pdf

Goldstein, Steven J., and Stein B. Jacobsen. "Rare Earth Elements in River Waters." *Earth and Planetary Science Letters*, vol. 89, no. 1, 1988, pp. 35–47., doi:10.1016/0012-821x(88)90031-3.

Gwenzi, W., Mangori, L., Danha, C., Chaukura, N., Dunjana, N., & Sanganyado, E. (2018). Sources, behaviour, and environmental and human health risks of high-technology rare earth elements as emerging contaminants. *Science of The Total Environment,636*, 299-313. doi:10.1016/j.scitotenv.2018.04.235

Hommen, U., & Rudel, H. (2012). Sensitivity analysis of existing concepts for application of biotic ligand models (BLM) for the derivation and application of environmental quality standards for metals and evaluation of the approaches with appropriate monitoring data sets from German waters. *Fraunhofer IME*. Retrieved January 16, 2019, from https://www.researchgate.net/publication/260337187_Sensitivity_analysis_of_existing_concepts_for_application_of_biotic_ligand_models_BLM_for_the_derivation_and_application_of_environmental_quality_standards_for_metals_and_evaluation_of_the_approaches_.

Iftekhar, S., Ramasamy, D. L., Srivastava, V., Asif, M. B., & Sillanpää, M. (2018). Understanding the factors affecting the adsorption of Lanthanum using different adsorbents: A critical review. *Chemosphere,204*, 413-430. doi:10.1016/j.chemosphere.2018.04.053

Kadirvelu, K., Kavipriya, M., Karthika, C., Radhika, M., Vennilamani, N., & Pattabhi, S. (2003). Utilization of various agricultural wastes for activated carbon preparation and application for the removal of dyes and metal ions from aqueous solutions. *Bioresource Technology,87*(1), 129-132. doi:10.1016/s0960-8524(02)00201-8

Kano, N., Pang, M., Deng, Y., & Imaizumi, H. (2017). Adsorption of Rare Earth Elements (REEs) onto Activated Carbon Modified with Potassium Permanganate (KMnO4). *Journal of Applied Solution Chemistry and Modeling,6*(2), 51-61. doi:10.6000/1929-5030.2017.06.02.1

Komnitsas, K., Zaharaki, D., Bartzas, G., & Alevizos, G. (2017). Adsorption of Scandium and Neodymium on Biochar Derived after Low-Temperature Pyrolysis of Sawdust. *Minerals,7*(10), 200. doi:10.3390/min7100200

Kotelnikova, A., Fastovets, I., Rogova, O., Volkov, D. S., & Stolbova, V. (2019). Toxicity assay of lanthanum and cerium in solutions and soil. *Ecotoxicology and Environmental Safety, 167*, 20-28. doi:10.1016/j.ecoenv.2018.09.117

Kulaksız, S., & Bau, M. (2013). Anthropogenic dissolved and colloid/nanoparticle-bound samarium, lanthanum and gadolinium in the Rhine River and the impending destruction of the natural rare earth element distribution in rivers. *Earth and Planetary Science Letters,362*, 43-50. doi:10.1016/j.epsl.2012.11.033

Kulaksız, S., Bau, M., Bau, M., Koschinsky, A., & Garbe-Schönberg, D. (2013). Rare earth elements as emerging contaminants in the Rhine River, Germany and its tributaries Andrea Koschinsky ; Dieter Garbe-Schönberg (Doctoral dissertation, Bremen, Jacobs Univ., Diss)

Kusrini, E., Kinastiti, D. D., Wilson, L., Usman, A., & Rahman, A. (2018). Adsorption of Lanthanide Ions from Aqueous Solution in Multicomponent Systems using Activated Carbon from Banana Peels (Musa paradisiaca L.). *International Journal of Technology,9*(6), 1132. doi:10.14716/ijtech.v9i6.2361

Lenntech. (n.d.). Biological Wastewater Treatment with Activated-Sludge Process. Retrieved January 10, 2019, from https://www.lenntech.com/wwtp/wwtp-overview.htm

Lerat-Hardy, A., Coynel, A., Dutruch, L., Pereto, C., Bossy, C., Gil-Diaz, T., . . . Schäfer, J. (2019). Rare Earth Element fluxes over 15 years into a major European Estuary (Garonne-Gironde, SW France): Hospital effluents as a source of increasing gadolinium anomalies. *Science of The Total Environment,656*, 409-420. doi:10.1016/j.scitotenv.2018.11.343

Lilia, M. (2015). Tertiary treatment of secondary effluents by Coagulation- ultrafiltration Comparative Study between two coagulants used: The Ferric Chloride and the Alum. *Recent Advances in Earth Sciences, Environment and Development,10*. Retrieved January 11, 2019, from https://www.researchgate.net/publication/323539905_Tertiary_treatment_of_secondary_effluents_by_Coagulation-_ultrafiltration_Comparative_Study_between_two_coagulants_used_The_Ferric_Chloride_and_the_Alum.

Louis, P. (2017). [Influent and Effluent Wastewater Composition]. Unpublished raw data.

Mohammed, R., & Chong, M. (2014). Treatment and decolorization of biologically treated Palm Oil Mill Effluent (POME) using banana peel as novel biosorbent. *Journal of Environmental Management,132*, 237-249. doi:10.1016/j.jenvman.2013.11.031

Muralikrishna, I., & Manickam, V. (2017). Wastewater Treatment Technologies. In *Environmental Management Science and Engineering for Industry* (pp. 249-293). Butterworth Heinemann. doi:10.1016/B978-0-12-811989-1.00012-9

Pagano, G., Guida, M., Tommasi, F., & Oral, R. (2015). Health effects and toxicity mechanisms of rare earth elements—Knowledge gaps and research prospects. *Ecotoxicology and Environmental Safety, 115,* 40-48. doi:10.1016/j.ecoenv.2015.01.03

Patel, H., & Vashi, R. (2015). Introduction. In *Characterization and Treatment of Textile Wastewater*(pp. 1-20). ScienceDirect. doi:10.1016/B978-0-12-802326-6.00001-0

Peirce, J. J., Weiner, R., & Vesilind, P. A. (1998). Wastewater Treatment. In *Environmental Pollution and Control*(4th ed.). doi:10.1016/B978-075069899-3/50009-2

Perlman, H., & USGS. (2016, December 2). Wastewater Treatment Water Use. Retrieved January 10, 2019, from https://water.usgs.gov/edu/wuww.html

Rabiet, M., Brissaud, F., Seidel, J., Pistre, S., & Elbaz-Poulichet, F. (2009). Positive gadolinium anomalies in wastewater treatment plant effluents and aquatic environment in the Hérault watershed (South France). *Chemosphere, 75*(8), 1057-1064. doi:10.1016/j.chemosphere.2009.01.036

Ramasamy, D. L., Puhakka, V., Repo, E., Hammouda, S. B., & Sillanpää, M. (2018). Two-stage selective recovery process of scandium from the group of rare earth elements in aqueous systems using activated carbon and silica composites: Dual applications by tailoring the ligand grafting approach. *Chemical Engineering Journal,341*, 351-360. doi:10.1016/j.cej.2018.02.024
Rare Element Resources. (2016). [Periodic Table with Rare Earth Elements Highlighted]. Retrieved January 15, 2019, from http://www.rareelementresources.com/rare-earth-elements#.XD2xZNJKjcs

The Water Treatment Process. (n.d.). Retrieved January 9, 2019, from https://www.bnl.gov/water/process.php

Tricca, A. (1998). Rare Earth Elements and Sr and Nd Isotopic Compositions of Dissolved and Suspended Loads from Small River Systems in the Vosges Mountains (France), the River Rhine and Groundwater. *Mineralogical Magazine,62A*(3), 1541-1542. doi:10.1180/minmag.1998.62a.3.142

Uehlinger, U., Arndt, H., Wantzen, K. M., & Leuven, R. S. (2009). The Rhine River Basin. *Rivers of Europe,*199-245. doi:10.1016/b978-0-12-369449-2.00006-0

United States Environmental Protection Agency. *Rare Earth Elements: A Review of Production, Processing, Recycling, and Associated Environmental Issues*(Rep.). (2012).

Voncken, J. H. L. *The Rare Earth Elements*. Springer Customer Service Center GmbH, 2016.

Zhao, H., Xu, X., Ke, F., Li, W., Feng, M., & Zhang, H. (2013). Nitrogen removal from wastewater plant secondary effluent in a compound natural treatment system. *Ecological Engineering,57*, 361-365. doi:10.1016/j.ecoleng.2013.04.026

Zhou, Y., Xing, X., Liu, Z., Cui, L., Yu, A., Feng, Q., & Yang, H. (2008). Enhanced coagulation of ferric chloride aided by tannic acid for phosphorus removal from wastewater. *Chemosphere,72*(2), 290-298. doi:10.1016/j.chemosphere.2008.02.028

Zhu, Y., Zheng, Y., & Wang, A. (2015). A simple approach to fabricate granular adsorbent for adsorption of rare elements. *International Journal of Biological Macromolecules, 72*, 410-420. doi:10.1016/j.ijbiomac.2014.08.039

Appendix A: Experimental Data Tables

Table A.1: Concentration of an identical cerium solution using two different preparation materials

Glass Bottles		Plastic Bottles	
Sample	**Concentration (μg • L^{-1})**	**Sample**	**Concentration (μg • L^{-1})**
1	3842.55	1	4057.59
2	3470.84	2	3954.43
3	3811.50	3	3995.20
4	3509.34	4	3900.98
5	3675.46	5	3837.46
6	3349.61	6	3952.78
7	3517.37	7	3759.14
8	3602.98	8	3813.82
9	3679.62	9	3897.80
10	3973.69	10	3793.16
11	3975.17	11	3824.16
12	3947.06	12	3818.49

Table A.2: Concentration of an identical neodymium solution over time using two different preparation materials

Glass Bottle Contact Time (min)	Concentration (μg • L^{-1})	Plastic Bottle Contact Time (min)	Concentration (μg • L^{-1})
0	3324.27	0	2867.33
1	2967.17	1	3522.80
2	2934.88	2	2993.61
3	2757.97	3	3091.92
4	2810.53	4	2975.36
5	2568.58	5	3281.75
6	3027.68	6	3196.91
7	2858.98	7	3164.00
8	3099.39	8	3185.99
9	2929.19	9	3123.31
10	2973.34	10	3161.34
15	3018.24	15	2989.70
20	3300.73	20	2788.83

Table A.3: Concentration of REEs in ultrapure water versus time using 0.05 g • L^{-1} of commercial activated carbon

Element	Activated Carbon Dose (g • L^{-1})	Type of Activated Carbon	Time (min)	Concentration (µg • L^{-1})
Nd	0.05	Commercial	0	2766.20
			15	2517.24
			30	2005.23
			45	2045.16
			60	2197.07
			120	2300.12
			180	2071.81
Yb	0.05	Commercial	0	2830.92
			15	1841.72
			30	1815.65
			45	1751.96
			60	1590.49
			120	1723.01
			180	1648.67
Gd	0.05	Commercial	0	3221.08
			15	2069.18
			30	2318.01
			45	1898.64
			60	2254.37
			120	1931.06
			180	2283.79
Ce	0.05	Commercial	0	2811.55
			15	2817.15
			30	2743.06
			45	2638.17
			60	2584.33
			120	3380.63
			180	2559.40
Tb	0.05	Commercial	0	2124.86
			15	1834.35
			30	1897.59
			45	1995.27
			60	1790.40
			120	1744.44
			180	1839.52

Table A.4: Concentration of REEs in ultrapure water versus time using 0.5 g • L^{-1} of commercial activated carbon

Element	Activated Carbon Dose (g • L^{-1})	Type of Activated Carbon	Time (min)	Concentration (μg • L^{-1})
Yb	0.5	Commercial	0	1713.66
			15	0.31
			30	12.31
			45	17.01
			60	24.60
			120	23.25
			180	17.46
Gd	0.5	Commercial	0	1609.38
			15	0.30
			30	6.42
			45	7.74
			60	11.14
			120	10.91
			180	9.36
Tb	0.5	Commercial	0	1605.90
			15	0.03
			30	0.90
			45	10.87
			60	12.09
			120	9.23
			180	9.07
Nd	0.5	Commercial	0	1774.83
			15	-0.26
			30	8.11
			45	9.04
			60	10.44
			120	2.61
			180	6.47
Ce	0.5	Commercial	0	2751.77
			15	-1.81
			30	5.52
			45	10.56
			60	6.76
			120	-13.21
			180	-7.73

Table A.5: Concentration of REEs in ultrapure water versus time using 2.5 g • L^{-1} of commercial activated carbon

Element	Activated Carbon Dose (g • L^{-1})	Type of Activated Carbon	Time (min)	Concentration (μg • L^{-1})
Nd	2.5	Commercial	0	1563.84
			15	17.18
			30	2.79
			45	0.53
			60	0.59
			120	0.23
			180	0.25
Yb	2.5	Commercial	0	1063.01
			15	17.67
			30	4.31
			45	2.05
			60	1.00
			120	0.45
			180	0.68
Gd	2.5	Commercial	0	1292.41
			15	34.99
			30	1.72
			45	0.81
			60	0.27
			120	-0.11
			180	0.01
Ce	2.5	Commercial	0	2374.93
			15	38.33
			30	11.47
			45	6.35
			60	4.23
			120	4.85
			180	3.41
Tb	2.5	Commercial	0	1238.54
			15	31.12
			30	0.95
			45	0.88
			60	0.20
			120	0.31
			180	0.11

Table A.6: Concentration of cerium in ultrapure water versus time using various doses of commercial activated carbon

Element	Activated Carbon Dose ($g \cdot L^{-1}$)	Type of Activated Carbon	Time (min)	Concentration ($\mu g \cdot L^{-1}$)
Ce	0.075	Commercial	0	2769.51
			15	1724.53
			30	1558.64
			45	1492.30
			60	1756.51
			120	1431.84
Ce	0.125	Commercial	0	1953.62
			15	1642.59
			30	1603.34
			45	1542.74
			60	1518.23
			120	1205.77
Ce	0.250	Commercial	0	2158.14
			15	457.70
			30	378.17
			45	2011.16
			60	1182.20
			120	225.15
Ce	0.375	Commercial	0	1775.53
			15	152.11
			30	113.51
			45	239.45
			60	42.84
			120	70.50

Table A.7: Concentration of REEs in ultrapure water versus time using 0.125 g • L^{-1} of commercial activated carbon

Element	Activated Carbon Dose (g • L^{-1})	Type of Activated Carbon	Time (min)	Concentration (µg • L^{-1})
Ce	0.125	Commercial	0	1953.62
			15	1642.59
			30	1603.34
			45	1542.74
			60	1518.23
			120	1205.77
Nd	0.125	Commercial	0	2240.17
			15	1163.21
			30	1148.50
			45	805.67
			60	1057.46
			120	392.21
Gd	0.125	Commercial	0	1237.37
			15	433.73
			30	417.82
			45	363.32
			60	324.18
			120	304.97
Tb	0.125	Commercial	0	491.74
			15	275.41
			30	252.86
			45	209.21
			60	231.76
			120	144.59
Yb	0.125	Commercial	0	2555.32
			15	-
			30	1832.33
			45	1635.11
			60	1055.57
			120	1463.59

Table A.8: Concentration of REEs in ultrapure water versus time using 0.125 g • L^{-1} of banana peel activated carbon

Element	Activated Carbon Dose (g • L^{-1})	Type of Activated Carbon	Time (min)	Concentration (µg • L^{-1})
Ce	0.125	Banana Peel	0	4487.44
			15	2839.44
			30	1984.85
			45	2101.64
			60	1582.52
			120	659.64
Nd	0.125	Banana Peel	0	2300.71
			15	1368.29
			30	1363.54
			45	1050.72
			60	1182.28
			120	850.12
Gd	0.125	Banana Peel	0	2124.84
			15	805.54
			30	665.37
			45	784.59
			60	645.86
			120	460.29
Tb	0.125	Banana Peel	0	1877.17
			15	1024.26
			30	817.91
			45	483.13
			60	481.44
			120	420.86
Yb	0.125	Banana Peel	0	2625.69
			15	1596.23
			30	891.41
			45	612.22
			60	599.90
			120	256.70

Table A.9: Concentration of cerium in ultrapure water versus time using 0.125 g • L^{-1} of various activated carbon types

Element	Activated Carbon Dose (g • L^{-1})	Type of Activated Carbon	Time (min)	Concentration (µg • L^{-1})
Ce	0.125	Commercial	0	1953.62
			15	1642.59
			30	1603.34
			45	1542.74
			60	1518.23
			120	1205.77
Ce	0.125	Banana Peel	0	4487.44
			15	2839.44
			30	1984.85
			45	2101.64
			60	1582.52
			120	659.64
Ce	0.125	Orange Peel	0	3705.07
			15	948.49
			30	434.97
			45	431.80
			60	162.38
			120	73.00

Table A.10: Concentration of equal parts cerium, gadolinium, and ytterbium mixed together in ultrapure water versus time using 0.125 g • L^{-1} of commercial activated carbon

Element	Activated Carbon Dose (g • L^{-1})	Type of Activated Carbon	Time (min)	Concentration (µg • L^{-1})
Ce	0.125	Commercial	0	711.08
			15	390.80
			30	517.77
			45	502.10
			60	470.79
			120	488.44
Gd	0.125	Commercial	0	768.61
			15	366.19
			30	446.72
			45	444.41
			60	434.99
			120	420.43
Yb	0.125	Commercial	0	754.07
			15	342.79
			30	422.80
			45	423.61
			60	427.65
			120	416.28

Table A.11: Concentration of equal parts cerium, gadolinium, and ytterbium mixed together in river water versus time using 0.125 g • L^{-1} of commercial activated carbon

Element	**Activated Carbon Dose (g • L^{-1})**	**Type of Activated Carbon**	**Time (min)**	**Concentration (µg • L^{-1})**
Ce	0.125	Commercial	0	274.67
			15	261.16
			30	264.99
			45	269.59
			60	261.23
			120	288.55
Gd	0.125	Commercial	0	322.18
			15	239.63
			30	229.32
			45	225.64
			60	221.09
			120	243.30
Yb	0.125	Commercial	0	348.12
			15	232.28
			30	219.69
			45	215.28
			60	209.85
			120	214.16

Table A.12: Concentration of equal parts cerium, gadolinium, and ytterbium mixed together in river water versus time using 0.125 g • L^{-1} of banana peel activated carbon

Element	**Activated Carbon Dose (g • L^{-1})**	**Type of Activated Carbon**	**Time (min)**	**Concentration (µg • L^{-1})**
Ce	0.125	Banana Peel	0	350.12
			15	307.89
			30	303.58
			45	300.14
			60	304.94
			120	310.97
Gd	0.125	Banana Peel	0	363.71
			15	304.92
			30	293.79
			45	272.19
			60	279.70
			120	274.06
Yb	0.125	Banana Peel	0	416.00
			15	335.11
			30	324.01
			45	293.73
			60	302.61
			120	291.72

Table A.13: Concentration of equal parts cerium, gadolinium, and ytterbium mixed together in ultrapure water versus time using 0.125 g • L^{-1} of banana peel biochar

Element	Activated Carbon Dose (g • L^{-1})	Type of Adsorbent	Time (min)	Concentration (µg • L^{-1})
Ce	0.125	Biochar	0	798.22
			15	437.05
			30	26.19
			45	24.66
			60	26.67
			120	29.51
Gd	0.125	Biochar	0	768.00
			15	467.33
			30	0.33
			45	-0.38
			60	0.48
			120	0.17
Yb	0.125	Biochar	0	715.12
			15	428.13
			30	-0.02
			45	-0.02
			60	-0.11
			120	-0.30

Table A.14: Adsorption capacity of commercial, banana peel, and orange peel activated carbon for various REEs

Type of Activated Carbon	Element	Adsorption Capacity (mg of REE • mg of adsorbent^{-1})
Commercial	Ce	0.00120
	Nd	0.00056
	Gd	0.00296
	Tb	0.00149
	Yb	0.00240
Banana Peel	Ce	0.00612
	Nd	0.00232
	Gd	0.00266
	Tb	0.00233
	Yb	0.00379
Orange Peel	Ce	0.00581

Table A.15: Concentration of gadolinium versus dose of $FeCl_3$ using two types of stock solution

Dose of $FeCl_3$ (mg • L^{-1})	**Concentration of Gd using 5x Stock Solution (µg • L^{-1})**	**Concentration of Gd using 5x Stock Solution (µg • L^{-1})**
0	-0.82	-0.71
1	2.95	3.13
2	6.57	4.59
3	5.74	4.89
4	6.44	5.84
5	6.12	3.98

Appendix B: Raw Data Tables

Table B.1: Raw data collected from ICP-AES showing concentration of REEs in ultrapure water versus time using 0.05 g • L^{-1} of commercial activated carbon

Element	Time (min)	Ce 535.353 {63} (Axial)	Nd 406.109 {83} (Axial)	Nd 430.358 {78} (Axial)	Nd 378.425 {89} (Axial)	Gd 335.047 {101} (Axial)	Gd 342.247 {98} (Axial)	Gd 310.050 {109} (Axial)
Nd	0	56.12	2791.03	2732.93	2774.64	28.00	13.90	16.76
	15	52.66	2502.72	2470.81	2578.20	10.38	-2.59	0.11
	30	44.99	1933.69	1918.82	2163.18	9.52	-1.81	0.10
	45	43.90	1967.06	1966.78	2201.64	12.90	1.42	3.48
	60	39.01	2068.18	2135.91	2387.12	12.23	-0.69	1.90
	120	48.57	2293.83	2327.62	2278.91	9.80	-2.20	0.21
	180	49.71	1974.27	2008.71	2232.45	10.46	-1.25	0.50
Yb	0	-359.92	9.63	7.87	9.35	0.79	0.93	0.30
	15	-796.73	2.61	-1.02	0.97	3.52	2.92	3.19
	30	-559.77	0.93	-1.83	-3.52	0.46	-0.08	0.50
	45	-720.41	1.85	-2.78	-1.10	6.58	5.96	6.48
	60	-866.56	0.63	-3.28	3.67	0.27	-0.07	0.20
	120	-561.05	0.73	-1.13	0.15	0.26	0.17	0.39
	180	-890.12	-0.98	-2.89	-1.54	1.21	-0.45	0.26
Gd	0	24.06	135.01	-2.04	15.15	3369.59	3082.39	3211.28
	15	28.66	81.16	-11.15	0.36	2160.29	1979.02	2068.23
	30	20.35	71.45	-14.02	-12.64	2421.02	2218.81	2314.20
	45	26.93	64.99	-13.58	-5.70	1981.72	1813.83	1900.37
	60	20.45	73.58	-14.47	-5.54	2224.01	2417.85	2121.24
	120	23.95	66.16	-14.58	-8.97	2007.35	1875.24	1910.58
	180	26.73	68.23	-15.70	-6.20	2397.37	2172.34	2281.67
Ce	0	2811.55	-0.30	-3.11	19.42	2.49	15.01	4.78
	15	2817.15	-9.25	-14.21	11.94	-0.32	12.87	1.55
	30	2743.06	-9.74	-12.95	13.40	-1.62	11.94	1.36
	45	2638.17	-2.01	-7.35	21.38	-1.00	11.55	1.23
	60	2584.33	-7.63	-11.92	11.54	5.88	18.05	7.26
	120	3380.63	-10.15	-15.37	13.37	-2.02	13.66	1.47
	180	2559.40	-7.32	-13.65	8.06	0.82	13.18	2.58
Tb	0	16.86	-63.04	5.14	36.09	12.97	9.98	0.41
	15	15.56	-55.94	-3.15	18.64	10.37	7.96	0.73
	30	22.11	-55.19	-4.05	24.35	10.45	8.39	0.97
	45	18.53	-58.25	-5.47	24.28	11.24	8.71	0.69
	60	7.79	-45.51	-1.06	19.05	10.89	7.33	0.42
	120	61.26	-49.52	-5.83	16.12	11.02	8.32	0.99
	180	16.91	-50.39	-4.27	15.82	10.21	7.49	0.44

Table B.1: (Continued)

Element	Time (min)	Tb 350.917 {96} (Axial)	Tb 332.440 {101} (Axial)	Tb 367.635 {92} (Axial)	Yb 328.937 {102} (Axial)	Yb 289.138 {116} (Axial)	Yb 297.056 {113} (Axial)
Nd	0	1.36	4.38	-19.98	5.47	5.27	4.80
	15	1.24	5.76	-18.24	4.84	4.59	4.46
	30	0.92	2.31	-14.63	7.40	7.35	6.79
	45	0.92	4.89	-16.11	4.79	4.28	4.49
	60	-0.16	5.44	-17.37	21.59	21.87	21.78
	120	0.85	6.20	-14.96	10.76	10.87	10.60
	180	0.58	3.73	-16.84	3.97	3.54	2.59
Yb	0	7.71	26.12	9.71	2647.27	2869.54	2975.97
	15	4.41	17.57	7.21	1569.35	1946.95	2008.85
	30	8.13	22.35	11.53	1788.18	1799.03	1859.75
	45	3.75	16.30	5.68	1599.06	1796.55	1860.27
	60	2.31	14.38	5.47	1435.68	1636.30	1699.48
	120	3.54	15.86	6.36	1387.56	1856.32	1925.15
	180	4.15	14.69	5.62	1511.28	1683.10	1751.61
Gd	0	-3.25	1.45	-8.77	2.00	1.03	-0.16
	15	-1.37	1.04	-4.50	1.42	0.50	-0.46
	30	-1.69	1.30	-3.96	1.24	0.32	-0.54
	45	-1.54	0.53	-4.38	0.89	-0.12	-1.40
	60	-1.69	0.38	-5.03	7.53	7.03	6.30
	120	-1.77	0.40	-5.05	1.92	0.76	-0.16
	180	-2.19	1.17	-3.56	1.17	0.27	-1.57
Ce	0	-11.23	-20.72	-3.67	0.09	-0.82	-2.00
	15	-10.97	-21.13	-3.69	0.95	0.06	-1.44
	30	-10.98	-20.94	-3.44	3.06	2.55	1.71
	45	-10.77	-21.29	-2.32	0.04	-0.94	-2.36
	60	-10.61	-18.05	-4.13	0.04	-0.90	-2.58
	120	-11.73	-23.40	-4.55	4.91	4.50	3.53
	180	-10.58	-21.68	-3.66	0.03	-0.73	-2.64
Tb	0	1873.37	2333.36	2167.84	0.07	3.33	-1.87
	15	1617.36	2012.29	1873.39	0.05	2.64	-2.26
	30	1672.68	2081.04	1939.06	0.01	2.90	-2.98
	45	1757.27	2190.25	2038.28	0.61	3.72	-2.18
	60	1575.12	1961.64	1834.43	0.60	3.15	-2.75
	120	1536.54	1910.37	1786.40	-0.02	2.71	-3.40
	180	1618.26	2020.32	1879.97	0.16	2.72	-3.48

Table B.2: Raw data collected from the ICP-AES showing concentration of REEs in ultrapure water versus time using 0.5 g • L^{-1} of commercial activated carbon

Element	Time (min)	Ce 535.353 {63} (Axial)	Nd 406.109 {83} (Axial)	Nd 430.358 {78} (Axial)	Nd 378.425 {89} (Axial)	Gd 335.047 {101} (Axial)	Gd 342.247 {98} (Axial)	Gd 310.050 {109} (Axial)
Yb	0	-433.932	18.617	19.895	35.193	2.644	3.816	3.260
	15	-10.939	-0.552	-0.828	5.755	0.114	-0.142	0.533
	30	-12.970	-0.953	0.229	0.062	0.403	0.312	-0.096
	45	-14.479	0.938	-1.867	3.885	-0.219	-0.449	-0.553
	60	-29.271	2.461	-1.509	-1.346	0.960	0.795	-0.762
	120	-30.979	-1.928	-1.177	-1.327	-0.492	0.311	-0.201
	180	-24.839	-0.226	-1.368	-0.084	0.448	-0.041	-0.631
Gd	0	-10.596	89.992	-5.726	18.297	1595.741	1608.596	1623.805
	15	-10.681	-1.126	-2.559	0.125	0.679	0.146	0.082
	30	-14.028	-1.643	-0.978	1.528	6.426	6.817	6.018
	45	-8.516	-0.939	-1.814	1.068	8.208	8.028	6.978
	60	-6.703	0.457	-1.418	-2.069	11.100	11.221	11.087
	120	-7.418	-2.931	-0.939	-0.372	10.945	10.702	11.077
	180	-14.987	-1.902	-1.570	-1.187	9.271	9.523	9.277
Tb	0	-10.523	-30.957	1.089	16.582	13.483	10.487	4.466
	15	-5.475	0.758	-2.826	1.501	0.180	0.457	0.115
	30	-13.032	-1.967	-1.886	-5.535	0.008	0.446	0.461
	45	-10.507	-1.441	-1.745	-4.961	0.364	0.335	0.159
	60	-8.554	-0.371	-2.669	-6.271	1.063	0.066	0.007
	120	-3.406	-0.579	-2.270	-3.812	0.847	0.660	-1.028
	180	-4.415	-0.076	-1.186	-1.310	1.120	0.523	-0.035
Nd	0	8.498	1660.06	1697.27	1967.16	10.508	-1.185	-0.593
	15	0.348	-0.670	-2.029	1.913	0.937	0.707	-0.136
	30	1.888	8.140	9.601	6.592	0.965	0.011	0.061
	45	-3.186	9.131	7.964	10.028	0.139	-0.353	-0.299
	60	2.380	10.438	9.723	11.172	1.063	0.371	0.084
	120	5.120	5.148	2.936	-0.247	1.163	0.102	-0.322
	180	-2.955	3.460	4.612	11.341	0.958	0.414	-0.065
Ce	0	2751.769	24.672	19.294	66.547	2.013	16.183	3.382
	15	-1.812	-1.977	-2.358	-4.485	0.477	-0.007	-0.776
	30	5.518	1.431	-3.308	-5.721	1.050	0.294	0.124
	45	10.560	-1.338	-2.835	0.061	0.898	0.232	0.134
	60	6.765	0.293	-2.782	-4.010	0.771	0.489	0.286
	120	-13.208	2.750	-2.727	0.613	0.449	0.139	-0.635
	180	-7.734	-0.851	-2.631	-4.413	0.967	0.105	-1.246

Table B.2: (Continued)

Element	**Time (min)**	**Tb 350.917 {96} (Axial)**	**Tb 332.440 {101} (Axial)**	**Tb 367.635 {92} (Axial)**	**Yb 328.937 {102} (Axial)**	**Yb 289.138 {116} (Axial)**	**Yb 297.056 {113} (Axial)**
Yb	0	4.929	19.009	3.021	1686.433	1725.085	1729.450
	15	-1.184	0.398	-0.399	0.374	0.573	-0.007
	30	-1.164	2.479	0.298	12.511	12.804	11.616
	45	-0.907	2.630	-1.649	16.901	17.561	16.569
	60	-1.433	4.046	-2.033	24.338	25.028	24.424
	120	-2.408	3.443	-2.618	23.191	23.874	22.690
	180	-1.297	3.403	-2.097	17.449	18.202	16.732
Gd	0	48.324	67.909	50.016	2.142	1.894	0.346
	15	-1.183	2.092	-1.266	0.011	0.277	-0.214
	30	-1.726	0.469	-1.456	0.026	0.257	-0.645
	45	-2.649	1.107	-1.351	0.007	0.364	-1.177
	60	-2.073	1.887	-1.133	0.023	0.530	-0.784
	120	-0.850	2.693	-1.378	0.059	0.295	-0.363
	180	-2.251	3.123	-2.743	0.140	0.388	-1.150
Tb	0	1454.372	1787.719	1575.619	0.309	3.324	-3.534
	15	-2.392	3.639	-1.147	-0.048	0.148	-0.103
	30	-0.021	3.034	-0.322	-0.016	0.207	-1.507
	45	8.277	14.511	9.821	0.038	0.115	-1.025
	60	8.045	17.288	10.934	-0.051	0.288	-0.927
	120	5.784	13.854	8.041	0.047	0.191	-0.752
	180	5.538	12.311	9.371	0.009	0.174	-1.191
Nd	0	-1.289	5.967	-16.964	8.569	8.726	8.283
	15	-3.558	3.369	-1.398	0.033	0.141	-0.780
	30	-1.652	2.313	-1.365	0.027	0.112	-0.747
	45	-2.746	-2.060	-2.779	0.038	0.177	-0.971
	60	-1.332	1.538	-1.147	0.003	0.267	-1.653
	120	-2.022	1.270	-1.546	0.045	0.033	-0.161
	180	-3.918	2.738	-0.578	0.211	0.114	-0.972
Ce	0	-10.397	-19.843	-4.129	0.655	0.838	-0.973
	15	-3.157	2.483	-1.403	-0.022	0.002	-1.342
	30	-1.099	2.303	-1.316	0.006	-0.037	-1.093
	45	-3.618	1.732	-1.942	-0.060	0.030	-1.251
	60	-3.232	1.517	-0.268	0.005	0.030	-1.002
	120	-3.285	2.474	-0.277	-0.004	0.342	-1.012
	180	-2.941	3.403	-1.809	-0.041	0.119	-0.851

Table B.3: Raw data collected from the ICP-AES showing concentration of REEs in ultrapure water versus time using 2.5 g • L^{-1} of commercial activated carbon

Element	**Time (min)**	**Ce 535.353 {63} (Axial)**	**Nd 406.109 {83} (Axial)**	**Nd 430.358 {78} (Axial)**	**Nd 378.425 {89} (Axial)**	**Gd 335.047 {101} (Axial)**	**Gd 342.247 {98} (Axial)**	**Gd 310.050 {109} (Axial)**
Nd	0	39.18	1509.60	1482.85	1699.06	13.12	3.35	4.76
	15	7.71	17.81	16.87	16.85	-0.05	0.20	-0.46
	30	9.54	4.05	3.50	0.83	0.16	0.02	-0.62
	45	2.35	0.78	0.32	0.48	0.84	0.37	-0.52
	60	4.27	1.46	0.09	0.22	0.18	0.20	-0.91
	120	4.91	0.15	0.19	0.35	0.12	0.24	-0.49
	180	0.02	0.96	0.80	-1.02	-0.06	0.35	-0.29
Gd	0	12.83	51.33	-7.32	2.54	1316.92	1259.14	1301.17
	15	9.74	1.40	1.08	-1.05	35.88	33.85	35.23
	30	8.77	0.96	0.46	-2.04	1.77	1.87	1.53
	45	8.67	-0.07	1.04	0.41	0.92	1.15	0.36
	60	7.78	0.66	0.01	-2.55	0.61	0.62	-0.40
	120	5.39	1.46	0.60	-1.19	0.16	0.60	-1.09
	180	5.82	0.05	-0.12	0.31	0.38	0.56	-0.91
Ce	0	2374.93	-7.54	-10.29	15.09	-1.20	11.50	-0.41
	15	38.33	0.38	-0.12	-1.22	0.40	0.39	-0.45
	30	11.47	2.34	-0.21	-5.92	0.49	0.19	-0.32
	45	6.35	-0.13	-0.51	-4.45	0.23	0.20	-0.37
	60	4.23	0.33	-0.66	-2.01	0.50	0.02	-0.36
	120	4.85	1.32	-0.15	-0.30	-0.67	0.05	-0.73
	180	3.41	0.62	-0.12	0.35	-0.13	0.51	-0.86
Tb	0	16.45	-37.62	-1.12	11.93	7.87	5.14	0.04
	15	6.57	0.01	0.29	-3.57	0.02	0.01	-0.81
	30	7.28	-0.11	-0.65	-2.81	0.49	-0.18	-0.43
	45	4.74	0.97	0.05	1.60	-0.11	0.18	-0.69
	60	10.17	0.74	0.08	-3.31	0.35	0.23	-0.40
	120	4.15	1.40	-0.47	0.79	0.38	0.16	-0.83
	180	-0.99	0.68	-0.08	0.70	-0.46	0.40	-0.29
Yb	0	-292.77	7.68	8.01	10.55	1.41	0.28	-0.48
	15	0.65	1.49	-0.50	-3.05	0.37	-0.20	-0.09
	30	3.32	0.38	-0.72	-3.51	0.20	0.23	-0.77
	45	7.05	1.67	-0.72	-1.86	-0.11	0.24	-1.14
	60	7.28	0.26	-0.36	-4.34	0.22	0.31	-0.80
	120	5.98	1.98	-0.82	-4.42	0.69	0.13	-1.06
	180	4.17	-0.80	0.26	-4.27	0.61	0.08	-1.45

Table B.3: (Continued)

Element	**Time (min)**	**Tb 350.917 {96} (Axial)**	**Tb 332.440 {101} (Axial)**	**Tb 367.635 {92} (Axial)**	**Yb 328.937 {102} (Axial)**	**Yb 289.138 {116} (Axial)**	**Yb 297.056 {113} (Axial)**
Nd	0	3.30	7.17	-8.58	3.52	3.35	3.29
	15	-0.19	-0.25	0.40	0.10	-0.14	-0.48
	30	0.49	0.06	0.10	0.02	0.05	-0.31
	45	-0.63	-0.15	-0.25	-0.03	-0.21	-0.48
	60	-0.61	1.88	-0.11	0.00	-0.11	-0.73
	120	-0.96	1.86	-0.64	0.00	0.13	-0.67
	180	-0.80	0.36	-0.95	0.00	0.21	-0.88
Gd	0	5.10	8.29	4.19	0.58	0.07	-0.70
	15	0.25	1.11	-0.34	-0.01	-0.40	-0.95
	30	-0.54	-0.28	0.35	-0.02	-0.22	-0.95
	45	-0.22	-0.91	-0.18	0.00	-0.24	-0.44
	60	-0.14	0.06	-0.79	0.01	-0.11	-0.59
	120	-0.79	0.10	-0.45	-0.01	-0.09	-0.69
	180	-0.36	0.34	-1.42	-0.03	-0.07	-0.77
Ce	0	-4.92	-12.66	1.89	-0.01	-0.45	-1.26
	15	-0.37	0.30	0.75	-0.01	-0.31	-0.52
	30	-1.50	0.78	-0.51	-0.01	-0.26	-1.08
	45	-0.11	-1.36	-0.47	-0.01	-0.45	-1.40
	60	-0.24	0.19	-0.89	-0.01	-0.25	-1.42
	120	-0.48	0.19	0.16	-0.03	-0.10	-1.13
	180	-0.85	1.36	0.09	0.06	0.09	-1.13
Tb	0	1075.60	1362.93	1277.09	0.19	2.15	-2.69
	15	26.27	35.88	31.22	0.01	-0.14	-1.44
	30	0.27	1.93	0.63	-0.02	-0.30	-1.04
	45	0.81	1.55	0.28	0.00	-0.46	-1.57
	60	-0.39	1.14	-0.14	0.02	-0.27	-1.36
	120	-0.40	1.53	-0.20	-0.02	-0.21	-1.46
	180	-0.78	1.39	-0.29	0.00	-0.07	-1.37
Yb	0	1.76	13.25	4.56	1010.73	1061.39	1116.90
	15	-1.35	0.75	-0.29	16.94	18.23	17.84
	30	-0.96	0.79	-0.67	4.58	4.72	3.62
	45	-0.49	0.34	0.80	2.52	2.32	1.32
	60	-1.33	1.03	-1.11	1.49	1.25	0.27
	120	-0.98	1.20	-0.57	1.06	0.89	-0.59
	180	-0.88	0.27	-0.73	1.32	1.39	-0.68

Table B.4: Raw data collected from the ICP-AES showing concentration of REEs in ultrapure water versus time using 0.125 g • L^{-1} of commercial activated carbon

Element	Time (min)	Ce 535.353 {63} (Axial)	Nd 406.109 {83} (Axial)	Nd 430.358 {78} (Axial)	Nd 378.425 {89} (Axial)	Gd 335.047 {101} (Axial)	Gd 342.247 {98} (Axial)	Gd 310.050 {109} (Axial)
Yb	0	-521.248	29.678	33.467	51.939	2.464	1.868	1.774
	30	-1194.462	8.665	7.944	19.451	54.507	54.891	56.761
	45	-545.726	2.996	3.518	15.383	32.423	32.400	32.134
	60	-489.107	0.241	3.462	9.449	24.538	25.122	25.471
	120	-1000.286	7.374	9.848	12.743	20.611	19.885	20.163
Gd	0	-10.178	136.470	-16.735	28.391	2224.904	2214.588	2281.031
	15	3.050	78.108	-1.711	26.643	1155.115	1138.969	1195.553
	30	-3.210	83.878	0.795	32.232	1240.209	919.673	1285.604
	45	1.131	75.449	-3.292	26.191	802.132	788.146	826.718
	60	-16.852	65.793	-4.427	21.000	1051.563	1037.049	1083.767
	120	-9.270	39.565	1.042	21.666	390.124	381.894	404.615
Tb	0	-2.847	-58.085	-2.268	2.647	15.103	13.569	8.613
	15	-21.007	-17.032	8.922	7.550	8.219	7.047	5.315
	30	176.599	-17.223	6.092	10.083	5.874	6.213	4.765
	45	185.836	-17.907	4.164	13.250	4.266	4.415	2.975
	60	-4.848	-14.841	4.756	6.104	6.196	5.073	4.553
	120	-6.987	-16.439	5.659	7.904	7.270	6.414	5.233
Nd	0	-7.535	463.444	475.626	536.165	6.069	2.242	3.423
	15	197.817	256.224	263.472	306.525	7.597	5.371	5.434
	30	184.359	239.711	241.530	277.353	3.210	2.855	2.693
	45	173.290	201.615	198.726	227.304	4.927	4.080	2.689
	60	-16.751	220.618	223.840	250.823	1.909	0.856	1.577
	120	178.264	199.534	5.437	228.801	2.861	1.301	1.721

Table B.4: (Continued)

Element	Time (min)	Tb 350.917 {96} (Axial)	Tb 332.440 {101} (Axial)	Tb 367.635 {92} (Axial)	Yb 328.937 {102} (Axial)	Yb 289.138 {116} (Axial)	Yb 297.056 {113} (Axial)
Yb	0	-4.607	20.042	-1.522	2417.592	2596.352	2652.004
	30	5.460	27.500	9.149	1790.626	1836.221	1870.130
	45	9.391	26.969	13.222	1772.579	1550.946	1581.807
	60	-1.611	16.356	5.401	1695.272	726.959	744.485
	120	1.813	15.994	3.942	1338.976	1508.021	1543.775
Gd	0	10.083	21.349	17.782	7.389	6.940	6.125
	15	15.304	27.920	20.954	11.262	11.190	11.237
	30	7.215	16.686	12.995	9.077	8.891	7.290
	45	12.111	20.247	17.108	8.389	8.388	7.402
	60	11.466	24.421	16.939	8.515	8.387	8.361
	120	3.078	13.928	8.969	4.663	4.578	3.535
Tb	0	1161.326	1413.162	1137.625	5.302	7.269	1.975
	15	392.141	483.452	425.610	6.582	7.581	4.724
	30	379.387	460.998	413.062	4.028	4.791	1.520
	45	328.802	403.063	358.104	2.005	2.868	-0.097
	60	292.562	362.237	317.752	3.291	3.992	1.327
	120	172.355	395.069	347.495	5.038	5.762	3.356
Nd	0	4.349	14.946	3.372	3.663	3.682	1.581
	15	-4.552	5.962	-2.222	5.991	5.976	4.308
	30	-3.495	4.640	-3.789	5.454	5.048	3.568
	45	-4.237	1.672	-3.586	2.253	1.817	-0.553
	60	-5.448	1.649	-2.993	2.093	1.925	-0.404
	120	-4.997	2.524	-5.078	2.569	2.694	0.883

Table B.5: Raw data collected from the ICP-AES showing concentration of REEs in ultrapure water versus time using 0.125 g • L^{-1} of banana peel activated carbon

Element	Time (min)	Ce 535.353 {63} (Axial)	Nd 406.109 {83} (Axial)	Nd 430.358 {78} (Axial)	Nd 378.425 {89} (Axial)	Gd 335.047 {101} (Axial)	Gd 342.247 {98} (Axial)	Gd 310.050 {109} (Axial)
Ce	0	4487.437	-86.804	-27.675	54.403	1.144	31.115	3.958
	15	2839.435	-43.810	-4.842	45.426	3.096	20.282	4.399
	30	1984.846	-39.133	-8.823	26.182	1.448	15.974	4.755
	45	2101.639	-41.219	-11.792	21.096	2.623	16.479	3.224
	60	1582.521	-30.100	-9.228	19.964	2.113	13.607	3.956
	120	659.639	-16.055	-1.984	7.509	0.049	4.977	0.735
Tb	0	31.967	-80.332	17.365	18.378	13.541	8.902	1.724
	15	24.532	-39.975	14.845	17.022	15.245	11.349	9.157
	30	23.063	-37.279	3.507	5.606	23.936	21.084	21.127
	45	27.614	-21.902	2.597	3.636	4.920	4.722	2.958
	60	33.686	-20.707	1.816	6.933	12.423	10.614	9.323
	120	29.581	-22.024	3.193	-1.178	9.663	7.933	5.834
Yb	0	-728.687	4.423	6.504	19.377	33.489	31.198	32.850
	15	-1046.797	14.755	13.122	22.656	48.455	45.549	48.852
	30	-706.738	5.858	7.002	10.196	20.426	19.260	19.371
	45	-400.572	5.108	8.725	12.614	8.183	8.982	9.463
	60	-369.302	15.988	21.614	32.180	12.415	12.787	14.054
	120	-138.275	2.689	2.821	-2.267	0.956	1.641	1.488
Gd	0	9.624	161.227	-10.934	35.010	2154.056	2024.032	2196.438
	15	17.311	69.633	5.512	25.247	820.260	766.973	829.372
	30	27.343	127.720	13.505	47.227	735.235	519.323	741.556
	45	22.278	72.475	7.668	29.675	799.687	741.470	812.600
	60	16.953	56.932	7.082	26.291	658.124	608.846	670.609
	120	20.099	39.855	7.189	14.626	470.165	434.201	476.492
Nd	0	42.310	1958.751	2379.522	2563.865	51.568	32.384	36.452
	15	18.755	1168.027	1410.254	1526.581	17.199	8.031	10.464
	30	16.267	1156.168	1411.852	1522.602	24.801	14.547	16.360
	45	19.121	911.148	1079.424	1161.576	17.534	9.348	9.687
	60	14.752	1003.774	1219.146	1323.917	23.496	14.604	15.158
	120	18.310	728.066	875.371	946.910	21.064	13.622	15.278

Table B.5: (Continued)

Element	Time (min)	Tb 350.917 {96} (Axial)	Tb 332.440 {101} (Axial)	Tb 367.635 {92} (Axial)	Yb 328.937 {102} (Axial)	Yb 289.138 {116} (Axial)	Yb 297.056 {113} (Axial)
Ce	0	-9.619	-32.171	-10.122	25.676	23.585	23.452
	15	-2.477	-12.335	-0.600	1.782	1.169	-0.020
	30	16.606	12.003	21.991	4.184	3.783	3.324
	45	6.335	0.715	9.722	1.568	1.059	0.280
	60	-2.014	-7.436	0.635	7.651	6.863	6.648
	120	4.786	6.877	9.648	0.529	-0.080	-0.240
Tb	0	1656.753	2041.324	1933.424	-0.914	2.646	-5.749
	15	902.968	1110.140	1059.671	23.094	23.933	20.731
	30	721.136	885.482	847.117	21.952	21.991	20.062
	45	425.061	526.226	498.111	7.021	7.410	5.092
	60	422.094	524.951	497.287	8.156	8.300	7.174
	120	370.503	457.304	434.780	7.960	8.256	6.529
Yb	0	-1.710	20.820	3.725	2455.080	2628.923	2793.062
	15	-1.419	14.628	2.467	1820.623	1440.993	1527.084
	30	-4.763	6.916	-0.889	1323.065	655.409	695.760
	45	-4.162	5.987	-1.844	545.689	624.956	666.006
	60	-1.933	9.550	-0.039	763.179	501.246	535.282
	120	-3.978	1.679	-0.067	261.536	246.060	262.515
Gd	0	-14.603	-7.961	-8.287	28.622	26.816	26.783
	15	-7.459	-3.852	-2.145	2.882	2.401	1.366
	30	-10.431	-4.346	-3.347	11.472	10.021	10.014
	45	-6.248	-1.157	-2.059	4.104	3.439	2.479
	60	-6.122	-2.051	-1.743	9.377	8.289	7.872
	120	-6.045	0.214	-2.590	2.883	2.234	1.630
Nd	0	1.673	10.840	-16.486	4.949	4.274	2.960
	15	-0.311	9.709	-9.563	30.581	28.619	29.272
	30	1.283	12.016	-7.588	38.912	36.764	37.158
	45	6.282	16.069	0.216	21.508	19.966	19.737
	60	1.441	10.249	-5.158	38.394	36.033	37.022
	120	0.575	10.831	-3.143	23.304	21.587	21.076

Table B.6: Raw data collected from the ICP-AES showing concentration of REEs in ultrapure water versus time using 0.125 g • L^{-1} of orange peel activated carbon

Element	Time (min)	Ce 535.353 {63} (Axial)	Nd 406.109 {83} (Axial)	Nd 430.358 {78} (Axial)	Nd 378.425 {89} (Axial)	Gd 335.047 {101} (Axial)	Gd 342.247 {98} (Axial)	Gd 310.050 {109} (Axial)
Ce	0	3705.067	-76.399	-24.745	44.312	0.624	26.190	3.665
	15	948.490	-19.241	-5.005	9.101	1.471	8.009	1.682
	30	434.973	-7.779	-3.609	5.240	-0.575	3.073	-0.300
	45	431.803	-9.419	-4.023	6.399	0.138	3.382	0.706
	60	162.384	-5.149	-2.493	-2.406	-0.583	1.068	-0.987
	120	73.001	-5.192	-1.653	-1.565	-1.232	0.537	-0.971

Table B.7: Raw data collected from the ICP-AES showing concentration of equal parts cerium, gadolinium, and ytterbium in ultrapure water versus time using 0.125 g • L^{-1} of commercial activated carbon

Element	Time (min)	Ce 535.353 {63} (Axial)	Nd 406.109 {83} (Axial)	Nd 430.358 {78} (Axial)	Nd 378.425 {89} (Axial)	Gd 335.047 {101} (Axial)	Gd 342.247 {98} (Axial)	Gd 310.050 {109} (Axial)
Ce Gd Yb	0	711.076	1.319	-21.519	-8.801	745.354	765.234	795.229
	15	390.798	40.432	-18.535	-28.601	357.870	360.952	379.737
	30	517.770	44.558	-22.973	22.529	432.033	438.444	469.672
	45	502.097	-3.144	-18.333	-27.984	429.273	439.395	464.567
	60	470.787	33.020	-17.368	-28.754	424.829	434.106	446.025
	120	488.444	41.845	-18.631	-12.690	414.206	413.791	433.299

Table B.7: (Continued)

Element	Time (min)	Tb 350.917 {96} (Axial)	Tb 332.440 {101} (Axial)	Tb 367.635 {92} (Axial)	Yb 328.937 {102} (Axial)	Yb 289.138 {116} (Axial)	Yb 297.056 {113} (Axial)
Ce Gd Yb	0	-12.481	-7.258	-9.990	748.642	750.838	762.728
	15	-11.550	9.900	2.824	339.582	341.484	347.301
	30	-9.866	-13.581	2.094	420.227	421.314	426.856
	45	-26.391	-17.288	-5.768	417.799	423.292	429.735
	60	-8.482	11.609	6.058	424.251	425.348	433.347
	120	-12.491	-3.325	-9.227	412.781	416.865	419.186

Table B.8: Raw data collected from the ICP-MS showing concentration of equal parts cerium, gadolinium, and ytterbium in river water versus time using 0.125 g • L^{-1} of commercial activated carbon

Element	Time (min)	Ce 535.353 {63} (Axial)	Nd 406.109 {83} (Axial)	Nd 430.358 {78} (Axial)	Nd 378.425 {89} (Axial)	Gd 335.047 {101} (Axial)	Gd 342.247 {98} (Axial)	Gd 310.050 {109} (Axial)
Ce Gd Yb	0	274.675	10.128	-8.991	9.941	343.925	305.290	317.321
	15	261.161	8.796	-6.536	10.643	255.662	225.675	237.547
	30	264.994	6.215	-7.671	11.792	245.529	215.358	227.064
	45	269.587	6.448	-8.444	6.877	241.015	211.583	224.332
	60	261.235	5.758	-7.872	8.381	237.453	207.877	217.944
	120	288.553	8.422	-6.994	6.263	260.610	227.693	241.587

Table B.8: (Continued)

Element	Time (min)	Tb 350.917 {96} (Axial)	Tb 332.440 {101} (Axial)	Tb 367.635 {92} (Axial)	Yb 328.937 {102} (Axial)	Yb 289.138 {116} (Axial)	Yb 297.056 {113} (Axial)
Ce Gd Yb	0	-1.738	-0.876	-3.050	357.597	331.001	355.753
	15	-1.747	-3.388	-2.985	238.657	219.980	238.200
	30	-1.914	-3.726	-2.685	225.646	207.336	226.098
	45	-2.599	-3.980	-1.941	221.164	203.009	221.656
	60	-1.526	-5.656	-1.924	215.522	198.212	215.808
	120	-1.943	-3.280	-2.978	220.307	202.015	220.163

Table B.9: Raw data collected from the ICP-MS showing concentration of equal parts cerium, gadolinium, and ytterbium in river water versus time using 0.125 g • L^{-1} of banana peel activated carbon

Element	**Time (min)**	**Ce 535.353 {63} (Axial)**	**Nd 406.109 {83} (Axial)**	**Nd 430.358 {78} (Axial)**	**Nd 378.425 {89} (Axial)**	**Gd 335.047 {101} (Axial)**	**Gd 342.247 {98} (Axial)**	**Gd 310.050 {109} (Axial)**
Ce Gd Yb	0	350.116	14.921	-9.067	16.821	389.255	337.862	364.018
	15	307.885	10.766	-9.684	9.101	327.271	284.076	303.407
	30	303.582	11.917	-8.995	6.758	314.960	273.852	292.548
	45	300.144	8.866	-8.087	11.537	292.466	254.068	270.026
	60	304.935	11.090	-9.709	8.620	301.288	260.664	277.150
	120	310.973	6.950	-8.693	7.671	295.283	255.796	271.112

Table B.9: (Continued)

Element	**Time (min)**	**Tb 350.917 {96} (Axial)**	**Tb 332.440 {101} (Axial)**	**Tb 367.635 {92} (Axial)**	**Yb 328.937 {102} (Axial)**	**Yb 289.138 {116} (Axial)**	**Yb 297.056 {113} (Axial)**
Ce Gd Yb	0	-2.075	-3.388	-2.779	428.593	390.789	428.633
	15	-1.765	-3.774	-2.275	345.634	315.071	344.635
	30	-1.817	-4.879	-2.870	333.756	304.949	333.333
	45	-2.099	-4.850	-2.867	302.871	276.084	302.224
	60	-2.618	-4.974	-2.206	312.558	284.071	311.213
	120	-3.037	-3.634	-3.330	301.309	273.762	300.092

Table B.10: Raw data collected from the ICP-AES showing concentration of equal parts cerium, gadolinium, and ytterbium in ultrapure water versus time using 0.125 g • L^{-1} of banana peel biochar

Element	**Time (min)**	**Ce 535.353 {63} (Axial)**	**Nd 406.109 {83} (Axial)**	**Nd 430.358 {78} (Axial)**	**Nd 378.425 {89} (Axial)**	**Gd 335.047 {101} (Axial)**	**Gd 342.247 {98} (Axial)**	**Gd 310.050 {109} (Axial)**
Ce Gd Yb	0	798.215	23.853	-6.317	24.18	780.373	761.337	762.3
	15	437.049	13.412	-5.619	5.046	477.057	457.542	467.396
	30	26.186	-0.989	-0.608	-3.791	0.838	0.116	0.032
	45	24.66	-0.792	-1.072	-1.971	0.322	-0.385	-1.081
	60	26.666	-0.395	-0.975	-5.324	0.647	0.295	0.499
	120	29.505	-0.056	-2.122	-7.333	0.599	-0.282	0.189

Table B.10: (Continued)

Element	**Time (min)**	**Tb 350.917 {96} (Axial)**	**Tb 332.440 {101} (Axial)**	**Tb 367.635 {92} (Axial)**	**Yb 328.937 {102} (Axial)**	**Yb 289.138 {116} (Axial)**	**Yb 297.056 {113} (Axial)**
Ce Gd Yb	0	-3.374	-2.595	-1.11	725.764	702.386	717.221
	15	-1.559	-0.634	1.354	431.812	419.56	433.028
	30	-1.621	1.227	0.162	0.24	0.132	-0.436
	45	-1.91	2.045	0.509	0.116	-0.09	-0.096
	60	-1.741	0.974	-0.127	0.123	-0.191	-0.255
	120	-1.295	0.081	0.261	0.093	-0.363	-0.634

Table B.11: Raw data collected from the ICP-AES of 3 tests showing concentration of gadolinium in synthetic wastewater versus dose of $FeCl_3$ using a 5x synthetic wastewater stock solution

Dose of $FeCl_3$	**Ce 535.353 {63} (Axial)**	**Nd 406.109 {83} (Axial)**	**Nd 430.358 {78} (Axial)**	**Nd 378.425 {89} (Axial)**	**Gd 335.047 {101} (Axial)**	**Gd 342.247 {98} (Axial)**	**Gd 310.050 {109} (Axial)**
0	47.15	0.791	-9.972	-1.182	-0.644	0.163	-2.187
1	44.925	0.314	-10.523	-6.504	3.133	3.655	2.161
2	44.758	-0.234	-9.714	-0.678	8.374	7.251	5.824
3	40.782	0.699	-9.768	-0.285	7.671	7.543	5.56
4	44.799	-0.561	-9.242	-3.599	7.171	7.478	5.831
5	47.943	1.372	-9.303	-5.687	7.645	6.333	5.824
0	50.49	1.448	-10.049	-6.147	-0.919	0.397	-1.038
1	47.557	0.834	-9.959	-6.918	3.229	3.511	1.921
2	46.002	1.214	-8.81	-2.902	5.761	6.703	5.045
3	43.656	2.209	-10.415	-3.568	5.775	5.385	3.713
4	50.465	0.548	-9.422	-2.244	7.692	7.021	5.947
5	51.143	1.329	-10.209	0.879	5.435	5.772	4.593
0	45.567	-0.251	-9.624	-2.551	-1.581	0.269	-1.85
1	52.324	1.335	-10.167	-2.561	3.812	3.567	1.525
2	44.925	1.112	-10.654	-5.048	7.27	6.91	6.034
3	52.465	-0.851	-8.846	-1.735	5.927	5.575	4.555
4	47.895	-0.484	-10.624	-1.77	6.502	5.538	4.81
5	48.508	0.64	-9.91	-3.22	7.511	6.721	5.22

Table B.12: Raw data collected from the ICP-AES of 3 tests showing concentration of gadolinium in synthetic wastewater versus dose of FeCl$_3$ using a 20x synthetic wastewater stock solution

Dose of FeCl$_3$	**Ce 535.353 {63} (Axial)**	**Nd 406.109 {83} (Axial)**	**Nd 430.358 {78} (Axial)**	**Nd 378.425 {89} (Axial)**	**Gd 335.047 {101} (Axial)**	**Gd 342.247 {98} (Axial)**	**Gd 310.050 {109} (Axial)**
0	47.15	0.791	-9.972	-1.182	-0.644	0.163	-2.187
1	44.925	0.314	-10.523	-6.504	3.133	3.655	2.161
2	44.758	-0.234	-9.714	-0.678	8.374	7.251	5.824
3	40.782	0.699	-9.768	-0.285	7.671	7.543	5.56
4	44.799	-0.561	-9.242	-3.599	7.171	7.478	5.831
5	47.943	1.372	-9.303	-5.687	7.645	6.333	5.824
0	50.49	1.448	-10.049	-6.147	-0.919	0.397	-1.038
1	47.557	0.834	-9.959	-6.918	3.229	3.511	1.921
2	46.002	1.214	-8.81	-2.902	5.761	6.703	5.045
3	43.656	2.209	-10.415	-3.568	5.775	5.385	3.713
4	50.465	0.548	-9.422	-2.244	7.692	7.021	5.947
5	51.143	1.329	-10.209	0.879	5.435	5.772	4.593
0	45.567	-0.251	-9.624	-2.551	-1.581	0.269	-1.85
1	52.324	1.335	-10.167	-2.561	3.812	3.567	1.525
2	44.925	1.112	-10.654	-5.048	7.27	6.91	6.034
3	52.465	-0.851	-8.846	-1.735	5.927	5.575	4.555
4	47.626	0.138	-5.753	-3.629	7.126	6.033	4.892
5	44.002	0.967	-8.634	1.564	3.938	4.175	3.424

Table B.13: Raw data collected from the ICP-AES of 3 tests showing concentration of gadolinium in wastewater versus dose of FeCl$_3$

Dose of FeCl$_3$	**Ce 535.353 {63} (Axial)**	**Nd 406.109 {83} (Axial)**	**Nd 430.358 {78} (Axial)**	**Nd 378.425 {89} (Axial)**	**Gd 335.047 {101} (Axial)**	**Gd 342.247 {98} (Axial)**	**Gd 310.050 {109} (Axial)**
0	-31.682	-1.88	-16.603	-2.513	-9.288	1.187	-15.258
1	-30.542	-0.815	-15.519	-1.435	-10.13	1.267	-16.262
2	-23.511	-2.108	-15.568	-3.272	-8.825	1.031	-15.344
3	-27.16	-1.238	-15.485	-4.29	-8.813	1.144	-15.278
4	-21.013	-0.718	-14.937	-3.467	-9.567	0.896	-15.954
5	-22.165	0.638	-16.425	-3.286	-9.296	1.182	-15.47
0	-25.401	-0.23	-15.979	-1.33	-9.418	0.941	-16.476
1	-25.425	-1.912	-16.977	-1.879	-7.425	0.896	-15.878
2	-19.139	-1.26	-15.384	-2.963	-9.305	1.447	-15.987
3	-20.749	-2.766	-15.506	4.102	-9.413	1.609	-16.412
4	-24.933	-1.734	-16.859	-1.978	-8.764	1.621	-16.581
5	-16.927	-1.548	-16.686	-0.568	-9.424	0.831	-16.099
0	-19.633	-3.552	-16.564	2.305	-10.383	1.494	-16.74
1	-13.498	-0.723	-16.359	2.457	-10.793	1.031	-17.003
2	-20.38	1.984	-16.353	-0.093	-9.803	1.147	-16.565
3	-16.746	-1.227	-16.348	-4.107	-9.945	1.849	-16.297
4	-13.731	-4.778	-16.709	-0.992	-9.815	0.983	-16.444
5	-16.26	-3.773	-17.831	-0.633	-9.661	1.167	-16.388

Table B.14: Raw data collected from the ICP-AES of 3 tests showing concentrations of equal parts cerium, gadolinium, and ytterbium in wastewater versus dose of $FeCl_3$

Dose of $FeCl_3$	**Ce 535.353 {63} (Axial)**	**Nd 406.109 {83} (Axial)**	**Nd 430.358 {78} (Axial)**	**Nd 378.425 {89} (Axial)**	**Gd 335.047 {101} (Axial)**	**Gd 342.247 {98} (Axial)**	**Gd 310.050 {109} (Axial)**
0	-17.747	0.808	-17.617	-0.842	-10.365	0.533	-17.155
1	-5.783	1.372	-17.274	1.167	-10.53	0.406	-18.028
2	-14.138	-0.473	-16.62	0.863	-10.317	1.362	-17.101
3	-12.851	0.479	-17.371	0.506	-10.645	0.786	-17.801
4	2.29	-0.102	-17.651	2.138	-10.895	1.114	-17.294
5	3.189	-1.154	-15.844	-1.937	-10.671	1.527	-16.761
0	0.848	-1.685	-15.199	-5.358	-12.059	0.458	-18.067
1	2.107	-1.246	-16.727	-3.842	-10.676	1.108	-18.319
2	-0.078	0.209	-16.329	-2.154	-10.941	0.798	-17.787
3	0.576	-0.177	-16.383	-0.246	-11.452	1.254	-17.618
4	2.167	-1.703	-16.925	-1.357	-11.069	0.954	-18.167
5	5.233	0.912	-16.389	0.913	-10.547	1.696	-17.368
0	-6.076	0.344	-16.094	-4.994	-11.568	0.361	-18.348
1	-3.403	-0.734	-16.803	-0.114	-10.897	0.717	-17.124
2	3.466	0.709	-17.322	-3.87	-10.805	1.437	-16.933
3	-2.427	-0.289	-17.257	0.981	-10.412	1.027	-17.757
4	-2.186	0.634	-16.808	-1.108	-11.444	1.083	-17.555
5	5.848	-2.615	-16.736	-2.256	-10.374	1.846	-16.942

Table B.14: (Continued)

Dose of FeCl$_3$	Tb 350.917 {96} (Axial)	Tb 332.440 {101} (Axial)	Tb 367.635 {92} (Axial)	Yb 328.937 {102} (Axial)	Yb 289.138 {116} (Axial)	Yb 297.056 {113} (Axial)	Tb 350.917 {96} (Axial)
0	-0.152	-0.578	-4.281	1.461	1.282	2.301	-0.152
1	-0.092	-1.952	-3.748	1.517	1.243	2.723	-0.092
2	0.47	-2.791	-4.748	1.706	1.298	3.29	0.47
3	-0.354	-0.84	-4.291	1.303	0.704	2.623	-0.354
4	0.023	-0.408	-3.742	1.416	1.234	2.44	0.023
5	0.07	-0.947	-3.854	1.341	1.039	2.586	0.07
0	0.218	-3.709	-3.64	1.545	1.264	2.229	0.218
1	0.017	-1.497	-4.417	1.762	1.26	2.705	0.017
2	-0.227	-1.279	-4.166	1.756	1.547	2.997	-0.227
3	0.294	-3.168	-3.35	1.535	1.265	2.586	0.294
4	-0.237	-1.623	-3.715	1.462	0.933	2.782	-0.237
5	-0.116	-0.863	-4.215	1.431	0.929	2.783	-0.116
0	-0.292	-0.925	-3.531	2.148	1.811	3.518	-0.292
1	-0.175	-0.453	-3.975	1.996	1.609	3.458	-0.175
2	0.297	-2.166	-3.257	1.721	1.153	2.958	0.297
3	-0.672	-2.494	-4.537	1.742	1.401	2.956	-0.672
4	0.619	-1.523	-4.794	1.512	1.062	2.953	0.619
5	-0.414	-1.23	-4.384	1.694	1.215	2.669	-0.414

Table B.15: Effluent concentrations of sodium, magnesium, calcium, and potassium in waste water samples (Batch 1).

Sample	Na ($\mu g \cdot L^{-1}$)	Mg ($\mu g \cdot L^{-1}$)	Ca ($\mu g \cdot L^{-1}$)	K ($\mu g \cdot L^{-1}$)
E2	66093	7891	77777	11376
E3	83923	8604	86396	11591
E4	70439	8097	85400	11306
E5	75508	8644	88250	12689
E6	86378	9909	101810	14986
E7	90949	9246	93517	13956
E8	98828	9209	93768	13323
E9	77451	9235	91557	12504
E10	76229	9533	97983	13183
E11	82973	9966	103980	12300
E12	95049	10049	110431	12274
E13	75160	9950	100637	10889
E14	83022	10769	114709	10293
E15	84485	11253	121725	10635
E17	90904	12237	131118	9165
E20	83650	11358	103461	14465
E22	74503	10540	88939	14120
E23	82549	11709	101386	14257
Average	82116.33	9900.01	99602.58	12406.26

Table B.16: Effluent concentrations of sodium, magnesium, calcium, and potassium in waste water samples (Batch 2).

Sample	**Na (μg • L^{-1})**	**Mg (μg • L^{-1})**	**Ca (μg • L^{-1})**	**K (μg • L^{-1})**
E1	84262	14963	85735	12421
E2	91553	16098	89939	15117
E3	98834	16458	86303	18693
E4	97362	16005	83749	18002
E5	91592	15697	80347	17042
E6	94631	15818	80687	17657
E7	101731	16115	79418	16724
E8	103431	15726	81294	17239
E9	97348	16080	82876	18754
E10	91262	15272	76008	18092
E11	101829	17600	90238	19888
E12	139854	18019	91420	20709
E13	102498	18542	93399	21103
E14	94638	18348	89947	20395
E15	107024	19179	94328	20688
E16	105162	18246	90417	18406
E17	108865	18824	95042	18391
E18	99505	18493	91039	18081
E19	98107	18250	88806	15856
E20	99888	17451	90246	13974
E21	89960	17304	96379	12004
E22	95247	17183	101493	11185
E23	99974	17284	99170	11799
E24	88815	17171	105140	11633
Average	99307.29	17088.53	89309.13	16827.16

Table B.17: Effluent concentrations of sodium, magnesium, calcium, and potassium in waste water samples (Batch 3).

Sample	**Na (µg • L^{-1})**	**Mg (µg • L^{-1})**	**Ca (µg • L^{-1})**	**K (µg • L^{-1})**
E1	85125	16644	92301	10649
E2	85217	17266	92924	11957
E3	84761	17824	87493	14629
E4	90390	18282	89827	15846
E5	89113	18083	80691	15984
E6	88771	18890	83389	16320
E7	108421	18403	81175	16647
E8	100477	18837	84061	16399
E9	102296	19031	83265	17103
E10	107089	18861	87877	17667
E11	105708	18486	86368	17864
E12	100017	18441	84309	18912
E13	98284	17687	81877	19781
E14	86035	17681	78194	17458
E15	85099	17765	78708	16449
E16	83143	18163	80678	16744
E17	82717	17841	81606	15229
E18	77404	17569	78264	15017
E19	81528	17109	80588	14164
E20	80517	17395	85699	13179
E21	82053	15700	88131	11806
E22	87335	15768	92698	11063
E23	91778	14384	97398	10058
E24	89007	14577	91044	8979
Average	90511.89	17528.57	85356.87	14996.06

Table B.18: Influent concentrations of nitrates, sulfates, chlorides, and phosphates in waste water samples (Batch 1).

Sample	NO_3 (mg • L^{-1})	SO_4 (mg • L^{-1})	Cl (mg • L^{-1})	PO_4 (mg • L^{-1})
E1	-	83.25	132.34	6.82
E2	-	75.88	94.85	4.36
E3	-	74.95	127.23	3.93
E4	-	76.09	105.90	4.18
E5	0.03	80.13	98.29	4.11
E6	0.24	81.55	111.27	5.07
E7	0.02	85.07	123.60	4.72
E8	-	83.55	133.88	4.87
E9	0.02	81.32	111.37	4.84
E10	-	81.24	112.24	4.63
E11	-	81.77	116.37	3.94
E12	-	84.34	126.67	4.36
E13	0.03	84.36	120.43	4.44
E14	0.06	83.26	127.14	3.22
E15	-	85.24	137.09	2.81
E16	0.03	84.24	144.25	2.59
E17	0.04	85.17	143.57	3.08
E18	-	-	-	-
E19	-	-	-	-
E20	-	84.97	130.46	8.82
E21	-	-	-	-
E22	0.04	85.26	113.51	8.38
E23	0.06	84.60	116.04	7.04
E24	-	-	-	-
Average	0.06	82.31	121.33	4.81

Table B.19: Influent concentrations of nitrates, sulfates, chlorides, and phosphates in waste water samples (Batch 2).

Sample	NO_3 (mg • L^{-1})	SO_4 (mg • L^{-1})	Cl (mg • L^{-1})	PO_4 (mg • L^{-1})
E1	-	133.3786	113.11754	1.96
E2	-	130.8462	123.09482	3.00
E3	-	135.3239	125.68224	3.83
E4	-	145.7476	131.14263	3.20
E5	-	129.1355	106.29836	2.55
E6	-	145.9418	117.51504	2.63
E7	-	140.7060	148.70993	2.40
E8	-	110.4902	107.64278	1.55
E9	-	112.3708	94.66780	1.45
E10	-	83.4846	67.74874	1.11
E11	-	116.9686	98.61051	1.49
E12	-	138.8746	182.67107	2.18
E13	-	142.9956	113.22942	2.10
E14	-	139.6582	114.31904	2.70
E15	-	139.9258	129.82106	2.18
E16	-	129.9964	131.97954	2.59
E17	-	139.9748	137.97989	2.26
E18	-	136.3109	115.86080	2.01
E19	-	123.4424	112.99013	2.01
E20	-	131.7714	120.23956	1.67
E21	-	99.1467	92.61853	1.03
E22	-	109.3203	114.75824	0.91
E23	-	130.8873	128.26213	1.50
E24	-	126.3996	124.57331	1.59
Average	-	128.04575	118.89721	2.07839

Table B.20: Effluent concentrations of nitrates, sulfates, chlorides, and phosphates in waste water samples (Batch 1)

Sample	**NO_3 (mg • L^{-1})**	**SO_4 (mg • L^{-1})**	**Cl (mg • L^{-1})**	**PO_4 (mg • L^{-1})**
S1	-	139.3694	140.58562	0.06
S2	-	143.7758	149.90593	0.09
S3	-	138.7407	148.15972	0.11
S4	-	143.8770	154.76218	0.16
Average	-	141.44	148.35	0.10

Table B.21: Effluent concentrations of nitrates, sulfates, chlorides, and phosphates in waste water samples (Batch 2)

Sample	**NO_3 (mg • L^{-1})**	**SO_4 (mg • L^{-1})**	**Cl (mg • L^{-1})**	**PO_4 (mg • L^{-1})**
S1	26.14083	85.8323	162.76644	1.11493
S2	23.72259	83.4621	161.44017	1.38863
S3	-	-	-	-
S4	19.12863	82.7814	149.21612	1.02976
S5	19.38229	82.1737	147.28665	0.89623
Average	22.09	83.56	155.18	1.11

Table B.22: Raw data collected from the ICP-MS showing concentration of elements in river water

Measurement	Concentration ($\mu g \cdot L^{-1}$)
139La (KED)	0.058769
140Ce (KED)	3.067872
141Pr (KED)	0.017972
146Nd (KED)	0.072114
147Sm (KED)	0.023193
151Eu (KED)	0.004545
152Sm (KED)	0.024873
153Eu (KED)	0.004599
157Gd (KED)	0.103312
158Gd (KED)	0.10491
159Tb (KED)	0.003163
161Dy (KED)	0.016369
163Dy (KED)	0.015949
165Ho (KED)	0.003383
166Er (KED)	0.010293
169Tm (KED)	0.001473
172Yb (KED)	0.119198
173Yb (KED)	0.118767
174Yb (KED)	0.119352
175Lu (KED)	0.001785

Appendix C: Supplementary Tables

Table C.1: Formula for synthetic wastewater treatment samples

Component	Concentration (mg • L^{-1})
Sodium	93.30
Magnesium	15.19
Calcium	100.25
Potassium	14.72
Phosphate	1.71

Table C.2: ICP-AES concentrations of elements in synthetic wastewater

Component	Concentration (mg • L^{-1})
Sodium	82.92
Magnesium	14.72
Calcium	6.45
Potassium	12.02
Phosphate	-

Appendix D: Sample Calculations

Concentration Calculations

In this example, magnesium sulphate heptahydrate ($MgSO_4 \bullet 7H_2O$) is used to reach the desired concentration of 15,190 µg of magnesium per liter.

Known:

$$MW_{\mathrm{MgSO4 \bullet 7H2O}} = 246.47\ \frac{g}{mol}$$

$$MW_{\mathrm{Mg}} = 24.31\ \frac{g}{mol}$$

$$MW_{\mathrm{SO4}} = 96.06\ \frac{g}{mol}$$

$$MW_{\mathrm{7H2O}} = 126.10\ \frac{g}{mol}$$

$C_{Mg} = 15{,}190\ \frac{\mu g}{L}$ (Desired Concentration)

$$C_{SO4} = C_{Mg} \bullet \frac{MW_{\mathrm{SO4}}}{MW_{\mathrm{Mg}}} = 15{,}190\ \frac{\mu g}{L} \bullet \frac{96.06\ \frac{g}{mol}}{24.31\ \frac{g}{mol}} = 60{,}035.03 \frac{\mu g}{L}$$

$$C_{7H2O} = C_{Mg} \bullet \frac{MW_{\mathrm{7H2O}}}{MW_{\mathrm{Mg}}} = 15{,}190\ \frac{\mu g}{L} \bullet \frac{126.10\ \frac{g}{mol}}{24.31\ \frac{g}{mol}} = 78{,}811.76 \frac{\mu g}{L}$$

$$Mass = Volume \bullet \left(C_{Mg} + C_{SO4} + C_{7H2O}\right)$$

$$Mass = 1\ L \bullet (15{,}190\ \frac{\mu g}{L} + 60{,}035.03 \frac{\mu g}{L} + 78{,}811.76 \frac{\mu g}{L})$$

$Mass = 154{,}036\ \mu g$ This is the amount of magnesium sulphate heptahydrate ($MgSO_4 \bullet 7H_2O$) that needs to be weighed to achieve 15,190 µg of magnesium per liter.

Adsorption Calculations

This example is for the maximum adsorption of Ce by BPAC at a 125 mg/L dose:

Knowns:

Initial Ce concentration: 4487.44 µg/L

Final Ce concentration: 659.64 µg/L

Percent reduction equation:

$$\%\ Reduction = \frac{Initial\ concentration - Final\ concentration}{Initial\ concentration} \bullet 100$$

Calculation:

$$\% \; Reduction\; Ce = \frac{4487.44\;\frac{\mu g}{L} - 659.64\,\frac{\mu g}{L}}{4487.44\;\frac{\mu g}{L}} \bullet 100$$

$$\% \; Reduction\; of\;\; Ce = 85.3\%$$

Activated Carbon Adsorption Capacity Calculations

In this example, we will calculate the adsorption capacity of BPAC for Ce

Knowns:

Initial Ce concentration, C_i: 4487.44 μg/L

Final Ce concentration, C_f: 659.64 μg/L

Volume of solution, V: 0.2 L

Weight of adsorbent, m: 125 mg

Adsorption capacity equation:

$$Q_c = \frac{\left(C_i - C_f\right) * V}{m}$$

Calculation:

$$Q_c = \frac{\left(4487.44\,\frac{\mathrm{\mu g}}{\mathrm{L}} - 659.64\,\frac{\mathrm{\mu g}}{\mathrm{L}}\right) * 0.2L}{125\; mg} * \frac{1\; mg}{1000\;\mathrm{\mu g}}$$

$$Q_c = 0.0061\;\frac{mg\; of\; REE}{mg\; of\;\; adsorbent}$$

Appendix E: Design Analysis

The urban wastewater treatment plant of Grand Nancy is responsible for treatment of wastewater for 60,000 people in the North-East of France (Pons et al, 2011). There are two parallel biological lines, each containing a reactor and a clarifier. The reactor, similar to a completely stirred tank reactor (CSTR), and the clarifier have respective volumes of 5,000 m^3 and 3,000 m^3. After these stages, the two lines combine to a tertiary treatment step for phosphorus removal. Recent analysis has shown a high concentration of Gd in the influent and effluent of the treatment plant at 3.0 mg • L^{-1} and 2.8 mg • L^{-1} respectively. MRI tracer dyes include Gd, and the REE is excreted by people in urine within 24 hours of injection. In accordance with the Urban Waste Water Treatment Directive of the European Union, the effluent concentration of Gd in wastewater discharges cannot exceed 0.4 mg • L^{-1} (European Commission, 2019) The managers of the plant decided to add $FeCl_3$ as a coagulant in their tertiary treatment to help remove the Gd.

$FeCl_3$ has been proven to remove REEs in wastewater treatment. The managers of the plant use previous experimental data to determine that they will dose their wastewater with 3 mg • L^{-1} of $FeCl_3$ solution in tertiary treatment for the effective removal of Gd. Previous treatment experiments revealed that at a pH of 4-7, the removal of REEs is optimal (Quinn et al, 2006; Anastopoulos et al, 2016). However, this is only desirable in small scale experimentation. WWTPs must maintain a neutral pH in order to be discharged back into the ecosystem. As a result, the cost to lower the pH for treatment, then to raise it for discharge is too high and unnecessary for the plant managers. The managers decided to omit this step of the treatment process. As a result, 3 mg • L^{-1} was determined to be the optimal dose for this plant's tertiary treatment phase.

Tertiary treatment can be altered to the specific needs of a treatment plant. In this design, the parallel biological lines will meet in a tank with a capacity of 20,000 m^3, where the water will be dosed with 60 kg of $FeCl_3$ to achieve the 3 mg • L^{-1} dose. Mixers in the tank will rapidly mix the solution for 20 minutes, followed by a flocculation period of 40 minutes, and finally a settling period of 180 minutes to allow for flocs to sufficiently settle to the bottom of the tank.

The Grand Nancy treatment plant already had the necessary equipment to complete the tertiary treatment. However, the $FeCl_3$ was an additional cost to the treatment process. Considering a dose of 3.0 $mg \bullet L^{-1}$ and the daily influent for the treatment plant to be 120 million liters per day, the total amount of $FeCl_3$ on a daily basis would be 360 kg. The average cost of $FeCl_3$ is about $551 per metric ton ($FeCl_3$ Price, 2018), therefore the total daily cost for the plant would be $198.36 without any bulk deals. This compounds to a yearly fee of $72,401.40 for the treatment plant.

Works Cited

Anastopoulos, I., Bhatnagar, A., & Lima, E. C. (2016). Adsorption of rare earth metals: A review of recent literature. Journal of Molecular Liquids,221, 954-962. doi:10.1016/j.molliq.2016.06.076

European Commission. (2019, February 12). Urban Waste Water Directive Overview. Retrieved February 18, 2019, from http://ec.europa.eu/environment/water/water-urbanwaste/index_en.html

FeCl3 Price. (2017). Retrieved January 25, 2019, from https://www.alibaba.com/showroom/fecl3-price.html

Pons, M., Mourot, G., & Ragot, J. (2011). Modeling and simulation of a carrousel for long-term operation. IFAC Proceedings Volumes,44(1), 3806-3811. doi:10.3182/20110828-6-it-1002.01018

Quinn, K. A., Byrne, R. H., & Schijf, J. (2006). Sorption of yttrium and rare earth elements by amorphous ferric hydroxide: Influence of pH and ionic strength. Marine Chemistry,99(1-4), 128-150. doi:10.1016/j.marchem.2005.05.011

Appendix F: Motive for Obtaining a Professional Engineer License

Being a Professional Engineer (PE) is a title obtained through hard work and diligence in both the classroom and out in the field. There are several steps that must be taken in order to obtain this license. Prospective PEs must first obtain a bachelors or masters engineering degree from an Adult Basic Education and Training (ABET) accredited four-year college. Next, they must pass the Fundamentals of Engineering exam. Afterwards, they need to complete four years of engineering experience under a licensed PE. Finally, the candidate is qualified to take the Principles and Practice of Engineering exam. In order to retain the PE license, the engineer must maintain and improve their skills throughout their career. Obtaining this license is an enormous benefit to any engineer, and should be a title sought out by any young engineer.

Professionally, the PE title opens many new doors and opportunities. Individuals holding this title are generally more sought after by employers. Only a licensed engineer can prepare, sign, seal, and submit engineering plans to a public authority for approval. Engineers holding a PE license typically earn higher wages than their unlicensed counterparts. From a legal standpoint, any engineer entering the consulting field is required to obtain a PE license. This holds true for engineers seeking to start a private practice as well. More flexibility becomes available in one's career, able to specialize in one particular field or maintain a broad career in engineering. The PE title also gives clients a sense of trust and security when they hire you for a job, offering a “stamp of approval” showing your hard work and effort towards the engineering community. Not only does the PE license provide professional benefits, there are many personal benefits offered by this title.

Obtaining the title of PE is held in high esteem within the engineering community. It carries respect and increased responsibility throughout an engineer’s career. This title shows the diligence and passion of an individual, and how they were driven to take the extra step to achieve this license. Some engineers believe they do not need a PE in their career; however, the future is unpredictable and it is unknown whether or not it will be needed in the future. For example, many states require individuals teaching engineering to have a PE license.

The PE license is the ultimate achievement for an engineer. This title grants an individual with many professional and personal benefits that are lasting throughout their lifetime. Obtaining a PE license is an objective that should be sought out by any young engineer, as it shows the dedication and excitement one holds for their profession.